

PAUL SCHERRER INSTITUT



Aeroradiometric Measurements in the Framework of the Swiss Exercise ARM13

Gernot Butterweck, Benno Bucher, Ladislaus Rybach, Georg Schwarz,
Eike Hohmann, Sabine Mayer, Cristina Danzi, Gerald Scharding

PSI Bericht Nr. 15-01
January 2015
ISSN 1019-0643

Aeroradiometric Measurements in the Framework of the Swiss Exercise ARM13

Gernot Butterweck¹, Benno Bucher², Ladislaus Rybach³, Georg Schwarz²,
Eike Hohmann¹, Sabine Mayer¹, Cristina Danzi⁴, Gerald Scharding⁴

- 1 Division for Radiation Safety and Security, Paul Scherrer Institute (PSI),
5232 Villigen PSI, Switzerland
- 2 Swiss Federal Nuclear Safety Inspectorate (ENSI), Industriestrasse 19,
5200 Brugg, Switzerland
- 3 Institute of Geophysics, Swiss Federal Institute of Technology Zürich (ETHZ),
8092 Zürich, Switzerland
- 4 Swiss National Emergency Operations Center (NEOC),
8044 Zürich, Switzerland

Paul Scherrer Institut (PSI)
5232 Villigen PSI, Switzerland
Tel. +41 56 310 21 11
Fax +41 56 310 21 99
www.psi.ch

PSI Bericht Nr. 15-01
January 2015
ISSN 1019-0643



ABSTRACT

The measurement flights of the exercise ARM13 were performed between June 24th and 27th, 2013. The exercise was organized by the National Emergency Operations Centre (NEOC) under coordination from the Expert Group for Aeroradiometrics (FAR). According to the alternating schedule of the annual ARM exercises, the environs of the nuclear power plants Gösgen (KKG) and Mühleberg (KKM) were surveyed. As in previous years, the distinction between pressurized and boiling water reactor is clearly identified from the photon spectra. Additional areas to the north and south of the routine measurement area of KKG and to the north-west of KKM were added during this exercise to improve information on the background radiation level.

Measurements over the cities of Biel/Bienne and Thun were performed in the program to obtain radiation background values over Swiss cities. Further areas in the Kander valley were added to the program of the exercise. All of these areas showed background-level readings.

A military training area near Thun was used to test parameters of the data evaluation and to intercompare air with ground measurements. A flight line from Berne to Zurich was used to increase the coverage of Switzerland with radiological measurements.

CONTENTS

1	INTRODUCTION	1
1.1	Measuring System	1
1.2	Measuring flights	2
1.3	Data evaluation	3
1.4	Data presentation	3
2	RESULTS OF THE MEASURING FLIGHTS	5
2.1	Recurrent measurement area KKG	6
2.2	Recurrent measurement area KKM	9
2.3	Biel/Bienne	12
2.4	Thun	15
2.5	Kander valley	18
2.6	Thun Military training ground	21
2.7	Flight Berne – Zurich	27
3	CONCLUSIONS	28
4	LITERATURE	28
5	PREVIOUS REPORTS	29
6	EVALUATION PARAMETER FILES	31
6.1	DefinitionFile_Processing.txt	31
6.2	DefinitionFile_DetC.txt	32

TABLES

Table 1: Quantification of the color scale	4
Table 2: Flight data of ARM13.....	5

FIGURES

Figure 1: Measurement system of the Swiss team.....	2
Figure 2: Super Puma Helicopter of the Swiss Air Force.	2
Figure 3: Dose rate in the vicinity of KKG.....	6
Figure 4: MMGC-ratio in the vicinity of KKG.....	7
Figure 5: ^{232}Th activity concentration in the vicinity of KKG.....	8
Figure 6: Dose rate in the vicinity of KKM.	9
Figure 7: MMGC-ratio in the vicinity of KKM.	10
Figure 8: ^{232}Th activity concentration in the vicinity of KKM.	11
Figure 9: Dose rate over Biel/Bienne city.	12
Figure 10: MMGC-ratio over Biel/Bienne city.	13
Figure 11: ^{232}Th activity concentration over Biel/Bienne city.	14
Figure 12: Dose rate over Thun city.	15
Figure 13: MMGC-ratio over Thun city.	16
Figure 14: ^{232}Th activity concentration over Thun city.	17
Figure 15: Dose rate in the Kander valley.	18
Figure 16: MMGC-ratio in the Kander valley.	19
Figure 17: ^{232}Th activity concentration in the Kander valley.	20
Figure 18: Vehicle equipped with gamma spectrometric equipment (left) and measurement with high pressure ionisation chamber (right).	21
Figure 19: Background dose rate at Thun military ground measured with a high pressure ionization chamber (RSS), NaI-based dose meter (AD-b) and airborne gamma spectroscopy (ARM).	22
Figure 20: Activity concentrations of the radionuclides ^{40}K , ^{232}Th and ^{137}Cs measured with in-situ gammaspectrometry on the ground and airborne gammaspectrometry at Thun military ground.....	22
Figure 21: Arial view of the Thun military ground, route of the gamma-spectroscopy vehicle and measured dose rate.	23
Figure 22: Comparison of the estimated source activity determined with airborne gamma spectrometry (ARM) at two source positions to the real source activity	24
Figure 23: Activity of a ^{60}Co source determined with airborne gamma spectrometry at different heights above ground.	25
Figure 24: Activity of a ^{137}Cs source determined with airborne gamma spectrometry at different heights above ground.	25

Figure 25: Activity of a ^{60}Co source determined with airborne gamma spectrometry at different heights above ground..... 26

Figure 26: Activity of a ^{137}Cs source determined with airborne gamma spectrometry at different heights above ground..... 26

Figure 27: Flight line of the measuring flight form Berne to Zurich. 27

Figure 28: Terrestrial dose rate along the profile from Berne to Zurich. 28

1 INTRODUCTION

Swiss airborne gamma spectrometry measurements started in 1986. Methodology and software for calibration, data acquisition and mapping were developed at the Institute of Geophysics of the Swiss Federal Institute of Technology Zurich (ETHZ). Between 1989 and 1993 the environs of Swiss nuclear installations were measured annually on behalf of the Swiss Federal Nuclear Safety Inspectorate (ENSI). This schedule was changed to biannual inspections in 1994, together with an organizational inclusion of the airborne gamma-spectrometric system into the Emergency Organization Radioactivity (EOR) of the Federal Office for Civil Protection (FOCP). The deployment of the airborne gamma-spectrometric system is organized by the National Emergency Operations Centre (NEOC). NEOC is also responsible for the recruitment and instruction of the measurement team. Aerial operations are coordinated and performed by the Swiss Air Force. The gamma-spectrometric equipment is stationed at the military airfield of Dübendorf. The gamma-spectrometry system can be airborne within four hours. Responsibility for scientific support, development and maintenance of the aeroradiometric measurement equipment passed from ETHZ to the Radiation Metrology Section of the Paul Scherrer Institute (PSI) in 2003 in cooperation with ENSI. General scientific coordination and planning of the annual measuring flights is provided by the Expert Group for Aeroradiometrics (FAR). FAR was a working group of the Swiss Federal Commission for NBC-protection (ComNBC) and consists of experts from all Swiss institutions concerned with aeroradiometry. FAR was re-organized as an expert group of the NEOC in 2008. Additional information can be found at <http://www.far.ensi.ch/>.

This report focusses on methodological aspects and thus complements the short report of NEOC about the annual flight surveys (available from the NEOC website).

1.1 Measuring System

The measuring system consists of four NaI-detectors with a total volume of 16.8 l. The spectrometer includes for each detector a 256-channel analyzer with automatic gain control. The measurement control, data acquisition and storage are performed with an industrial grade personal computer. A second, identically configured PC is present in the electronics rack (Figure 1) as redundancy. Under normal operation conditions, this PC is used for real-time evaluation and mapping of the data. The positioning uses GPS (Global Positioning System) in the improved EGNOS (European Geostationary Navigation Overlay Service) mode. Together with spectrum and position, air pressure, air temperature and radar altitude are registered. The measuring system is mounted in an Aérospatiale AS 332 Super Puma helicopter of the Swiss Air Force (Figure 2). This helicopter has excellent navigation properties and allows emergency operation during bad weather conditions and nighttime. The detector is mounted in the cargo bay below the center of the helicopter. The cargo bay is covered with a lightweight honeycomb plate to minimize photon absorption losses.

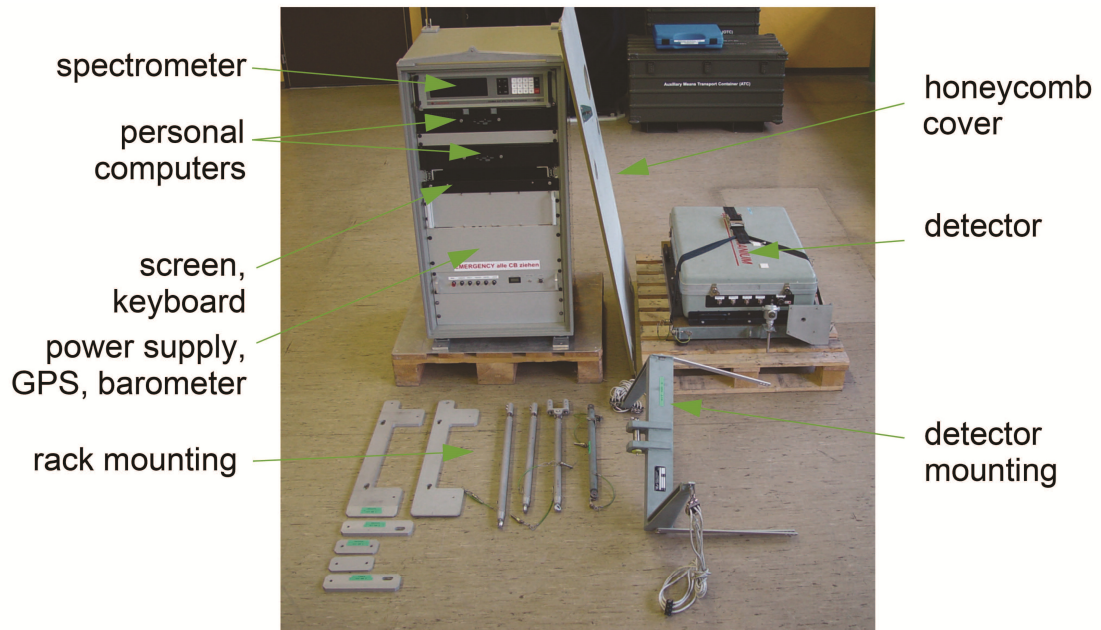


Figure 1: Measurement system of the Swiss team.



Figure 2: Super Puma Helicopter of the Swiss Air Force.

1.2 Measuring flights

The advantage of aeroradiometric measurements lies in the high velocity of measurements in a large area, even over rough terrain. Uniform radiological information of an area is obtained from a regular grid of measuring points. This grid is composed from parallel flight lines which are 100 m to 500 m apart, depending on the scope of

the measurement. The flight altitude above ground is aspired to be constant during the measuring flight. Typical values lie between 50 m and 100 m above ground. The spectra are recorded in regular time intervals of typical one second, yielding integration over 28 meters of the flight line at a velocity of 100 km/h.

1.3 Data evaluation

The data evaluation follows the methodology described in Schwarz (1991). Since the year 2000, software developed by the Research Group for Geothermics and Radiometry of the Institute of Geophysics of the Swiss Federal Institute of Technology Zurich (ETHZ) with on-line mapping options (Bucher, 2001) is used.

1.4 Data presentation

A first brief report (Kurzbericht) of the measurement results is compiled by the measurement team and published immediately after the end of the exercise on the homepage of NEOC. These reports are archived at <http://www.far.ensi.ch>.

Results of a further data evaluation are published in the form of a PSI-report. For all measuring areas, a map of the total dose rate and the flight lines is presented together with a map of the Man-Made-Gross-Count (MMGC) ratio. As the MMGC-ratio is a very sensitive measure for the presence of artificial radionuclides, false positive values occur and have to be identified. Thus, in former reports, a map of the variation of the count rate in the MMGC high-energy window was introduced for rapid information on the quality of the MMGC-ratio. Unfortunately, this additional map failed to cover artefacts in the MMGC-ratio map completely and led additionally to the confusion of some readers. Starting with this report, the count rate map of the MMGC high energy window is abandoned in favor of using a less sensitive color scale of the MMGC-ratio map, even if this renders the comparison with former reports more difficult.












A map of the ^{232}Th activity concentration yields quality information as it can be expected that this quantity is constant over time. As an additional quality measure, an appendix with the basic parameters of the data evaluation is added to simplify a re-evaluation of the data in the future.

If the MMGC-ratio indicates elevated values, maps of individual radionuclides are added based on the average photon spectrum over the affected area.

In the case of large changes of topography in the measured area, a map of the terrestrial dose rate consisting of the total dose rate reduced of the altitude dependent cosmic component is included. In the case of measuring flights with the main purpose of mapping natural radionuclide concentrations, a supplementary map of the ^{40}K activity concentration is presented.

All maps use a gradual color scale from blue for low values to red for high values. The maximum and minimum values are specified in the legend together with the measurement unit of the depicted quantity. The colors for 10 percent steps between minimum and maximum values of the scale are given in Table 1.

Table 1: Quantification of the color scale

Percentage	Color
≥ 100	
90	
80	
70	
60	
50	
40	
30	
20	
10	
≤ 0	

2 RESULTS OF THE MEASURING FLIGHTS DURING THE EXERCISE ARM13

The flights of the exercise ARM13 were performed with a Super Puma helicopter of the Swiss air force between June 24th and 27th. The helicopter was refurbished in a program of the Swiss air force, requiring small changes in the mechanical support of the detector and connections between helicopter and ARM system. Personnel of the military unit Stab BR NAZ performed the measurements supported by experts from ENSI, PSI and NEOC. Representatives of KomZenABC-Kamir and of Labor Spiez participated in the measurements at Thun military ground, see Chapter 2.6. A short report with preliminary measurement results was placed on the NEOC website <https://www.naz.ch/> on June 28th, 2013. Flight parameters of ARM13 are listed in Table 2. Flight velocity of all measuring flights was around 30 m/s with a ground clearance of 90 m. The counting interval of the spectra was one second.

Table 2: Flight data of ARM13

Location	Flight number	Date	Effective measuring time [s]	Length of run [km]	Area [km ²]
KKG	2013007 2013008 2013009	24.6.2013	16274	801	468
KKM	2013012 2013015	25.6.2013	10140	560	296
Biel/Bienne	2013014	25.6.2013	4127	216	55
Thun	2013016 2013019	26.6.2013	2045	94	23
Kander Valley	2013018	26.6.2013	3430	117	42
Thun military training ground	2013020 2013021 2013022 2013023 2013027 2013028 2013029 2013030 2013031	27.6.2013		10	2
Flight Berne - Zurich	2013032	27.6.2013	3615	196	-

2.1 Recurrent measurement area KKG

According to a biannual rotation of routine measurements, the environs of the nuclear power plant Gösgen (KKG) were inspected in 2013. Areas to the north and south of the routine measurement area of KKG were added during this exercise to improve information on the background radiation level. The dose rate map (Figure 3) shows values in the normal background range.

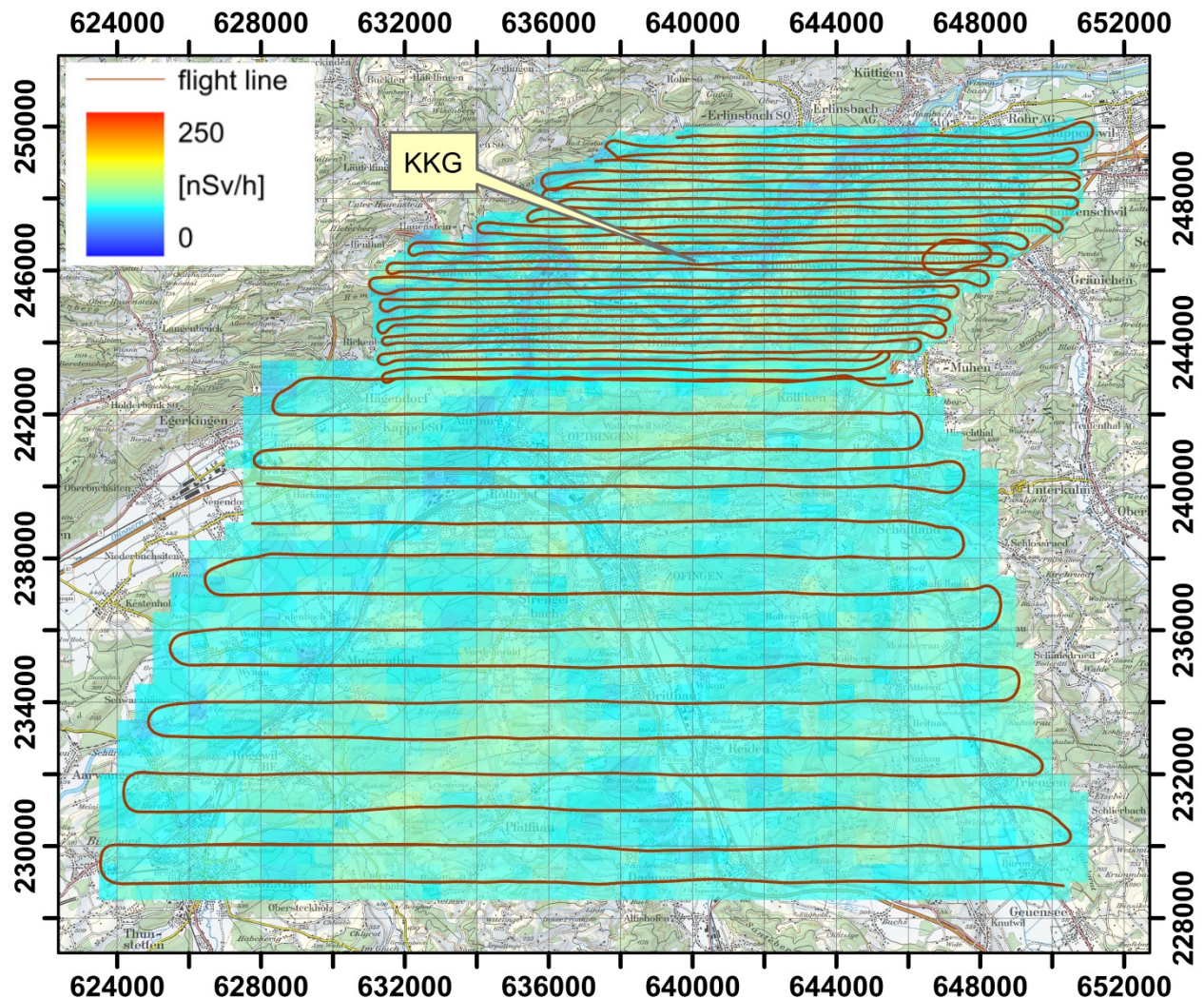


Figure 3: Dose rate in the vicinity of KKG. PK100 © 2013 swisstopo (JD100042)

The environs near KKG were measured with a 250 m spacing of the flight lines, whereas for the area to the south a spacing of 1000 m was used. From the spectra along the flight lines, values are interpolated to a grid raster for mapping. The optimal cell size for this process is half the line spacing. Thus, the areas measured with different line spacing were projected to two different grids with cell sizes of 125 m and 500 m, respectively. The grids are plotted slightly transparent to show the underlying topographical map. Due to the superposition in overlapping parts of the grids this transparency is reduced. This is clearly observable in the map of the MMGC-ratio (Figure 4). No indication of artificial radionuclides was detected.

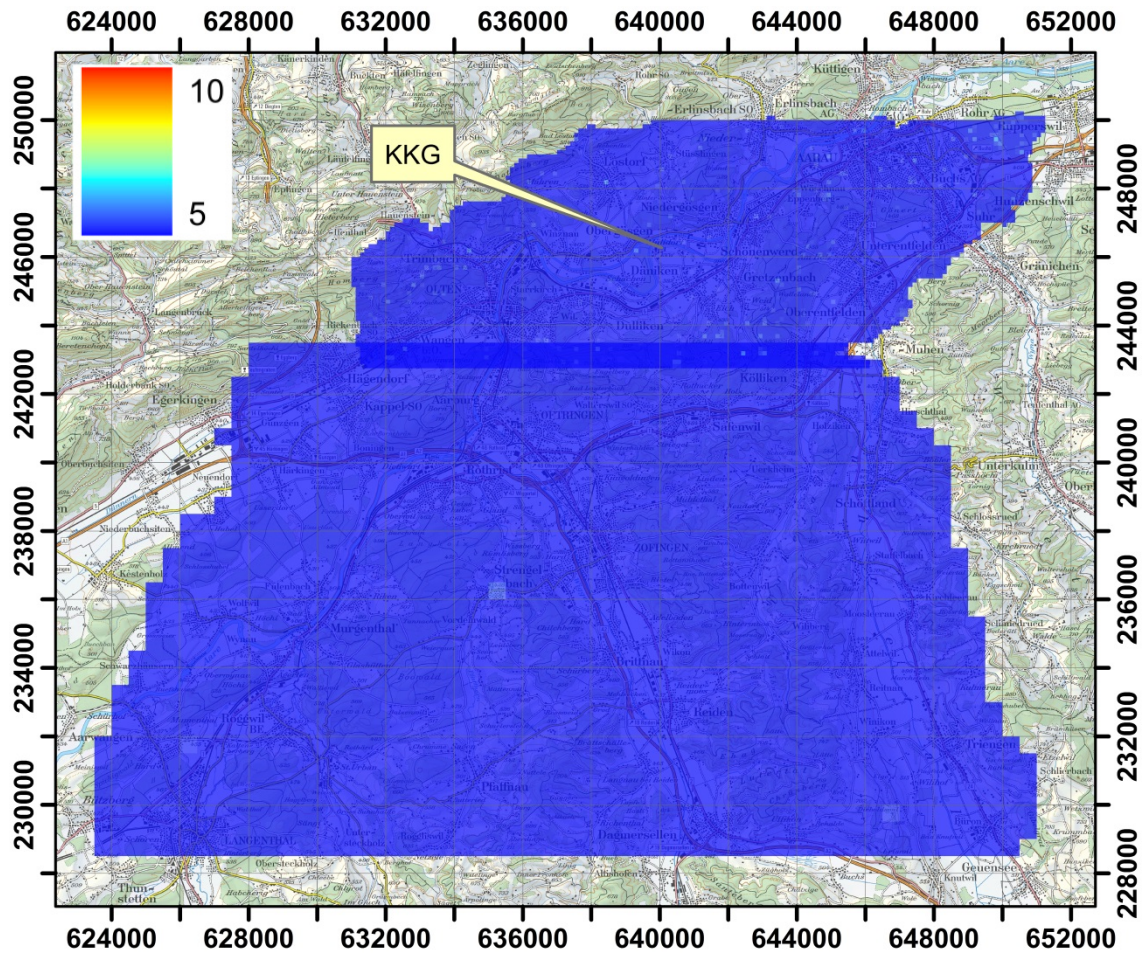


Figure 4: MMGC-ratio in the vicinity of KKG. PK100 © 2013 swisstopo (JD100042)

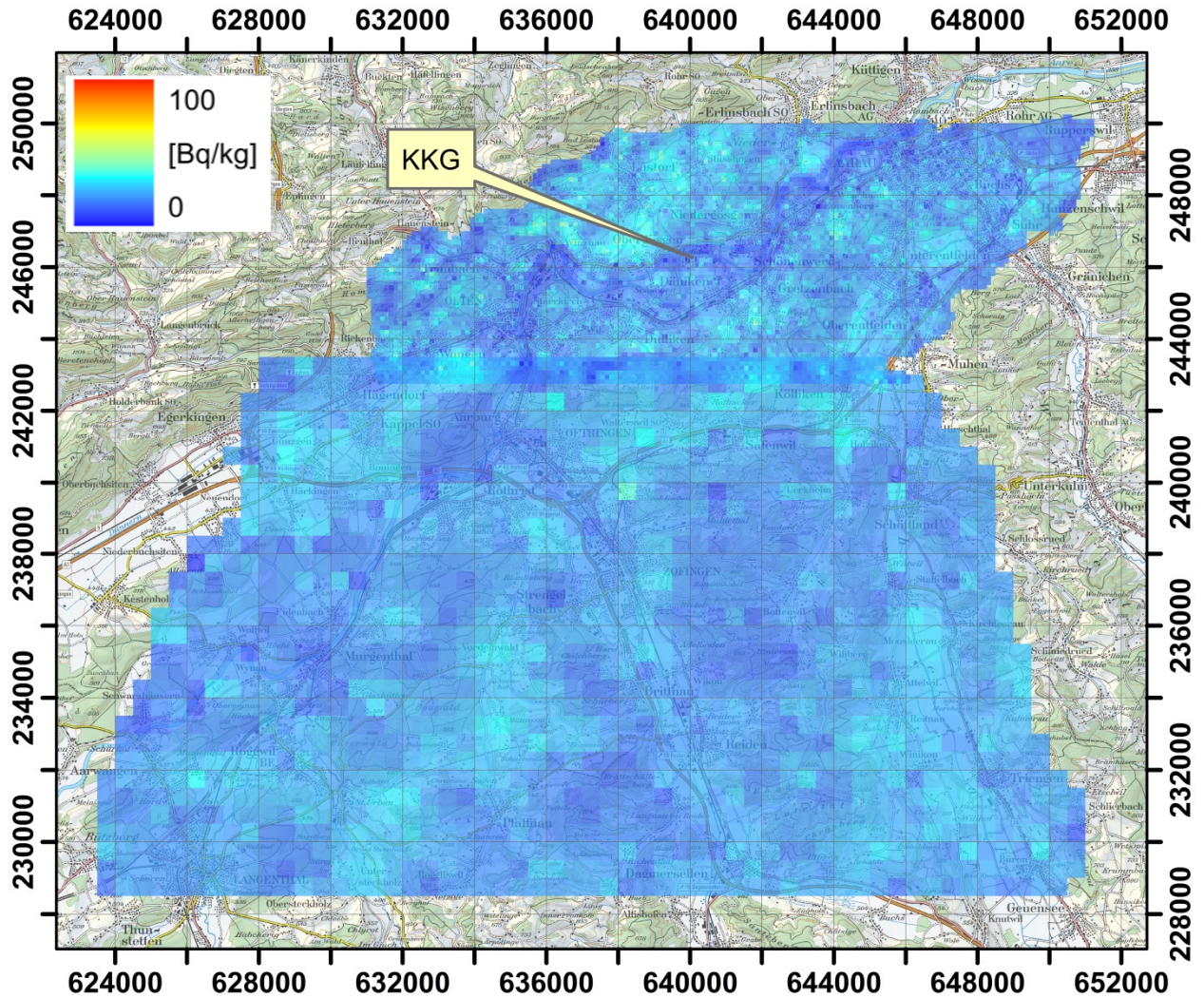


Figure 5: ^{232}Th activity concentration in the vicinity of KKG. PK100 © 2013 swisstopo (JD100042)

The map of ^{232}Th activity (Figure 5) concentration yields lower values over regions where photon emissions from soil and rock are absorbed by layers of water.

2.2 Recurrent measurement area KKM

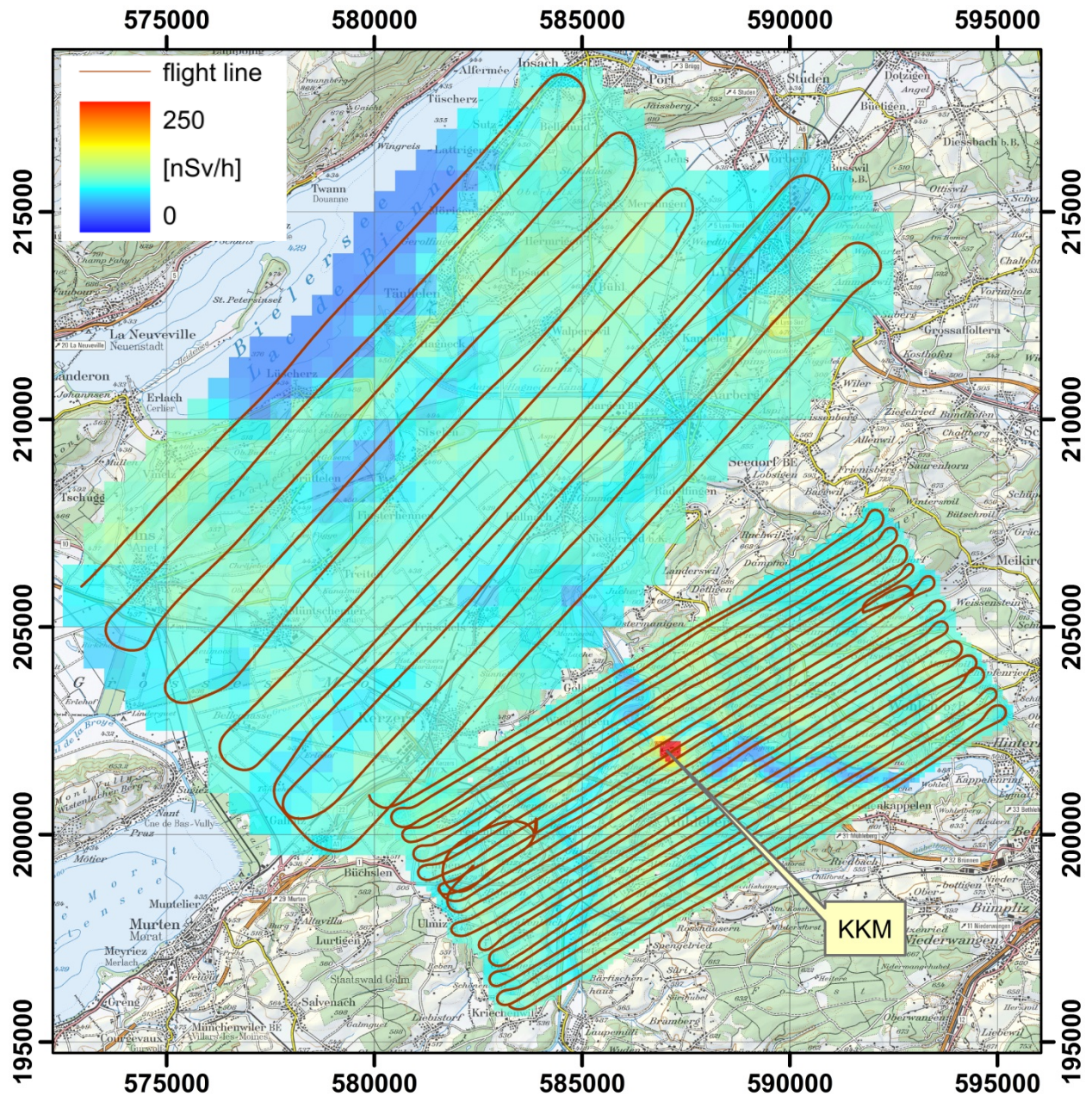


Figure 6: Dose rate in the vicinity of KKM. PK100 © 2013 swisstopo (JD100042)

According to a biannual rotation of routine measurements, the environs of the nuclear power plant Mühleberg (KKM) were inspected in 2013. An area to the north-west of the routine measurement area of KKM was added during this exercise to improve information on the background radiation level. The dose rate map (Figure 6) and the map of the MMGC-ratio (Figure 7) show values in the normal background range outside of the plant premises. Elevated values over the plant are due to the nuclide ^{16}N . This nuclide is transported in a boiling water reactor with the primary steam to the turbines in the engine building. The roof of the engine building is less shielded than

the reactor building and the high energy photon radiation of ^{16}N can thus be detected from above.

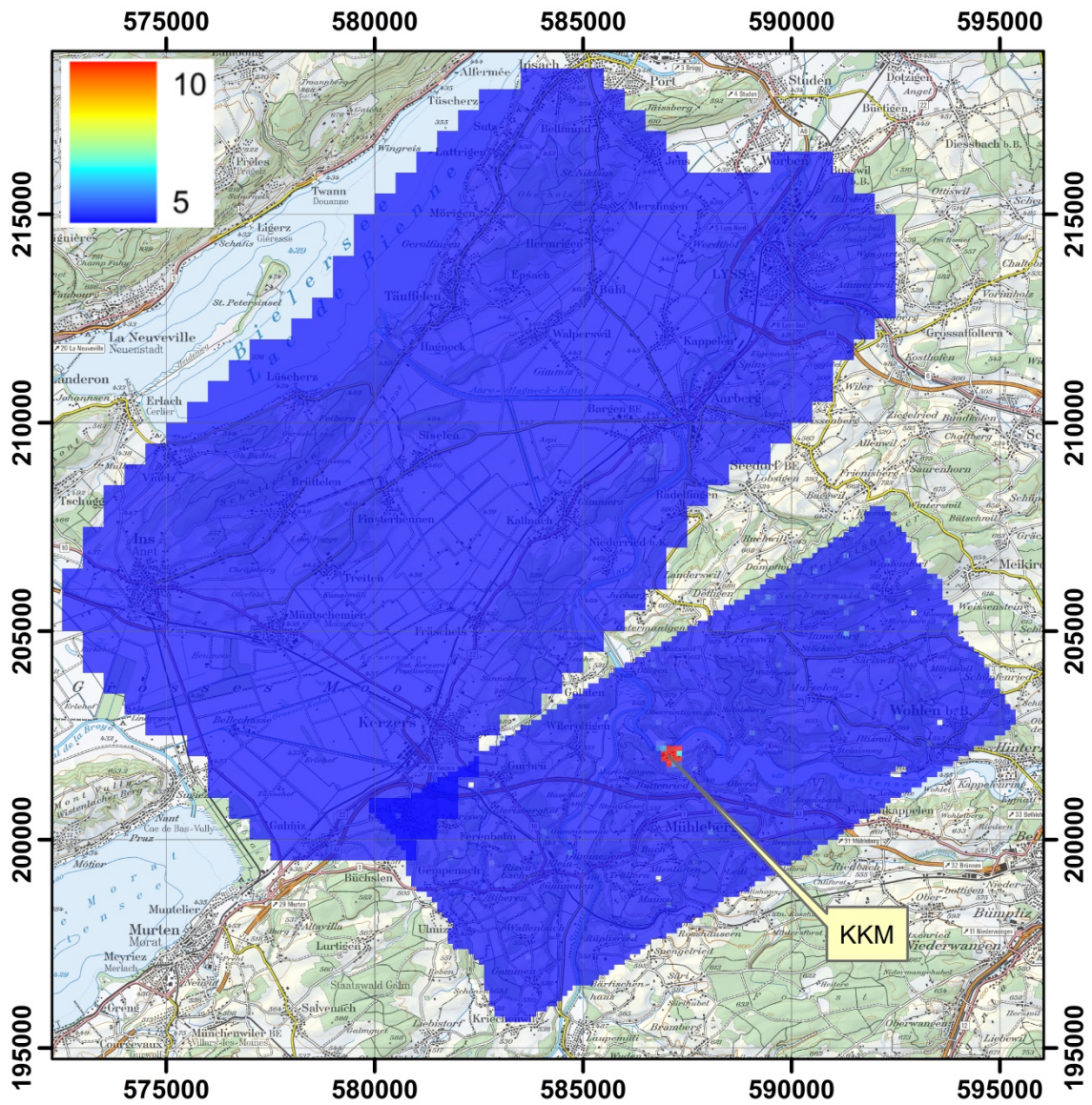


Figure 7: MMGC-ratio in the vicinity of KKM. PK100 © 2013 swisstopo (JD100042)

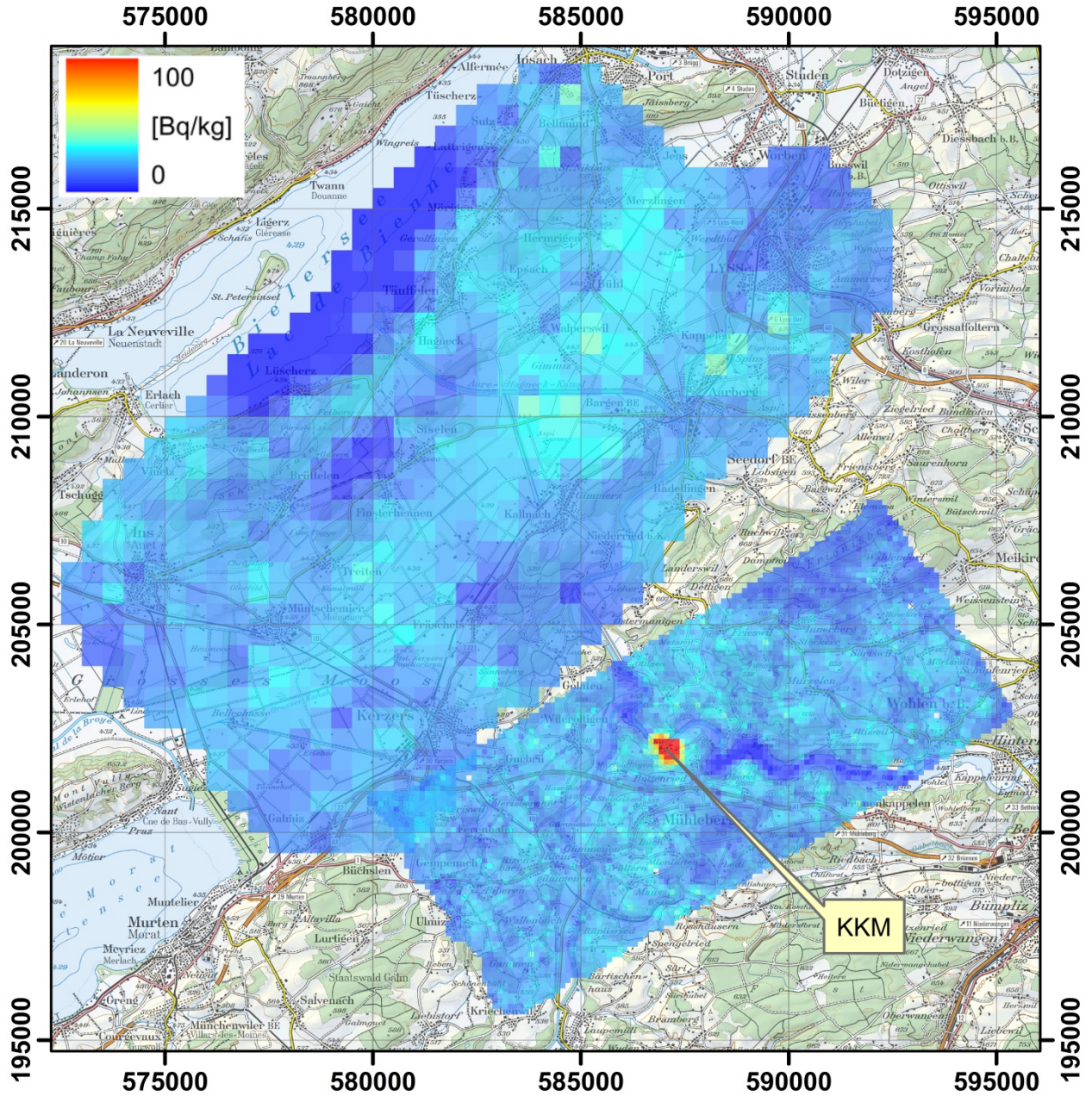


Figure 8: ^{232}Th activity concentration in the vicinity of KKM. PK100 © 2013 swisstopo (JD100042)

The map of the ^{232}Th activity concentration (Figure 8) shows elevated values over the KKM plant premises. This is due to a misinterpretation of scattered high energy photon radiation of the nuclide ^{16}N .

2.3 Biel/Bienne

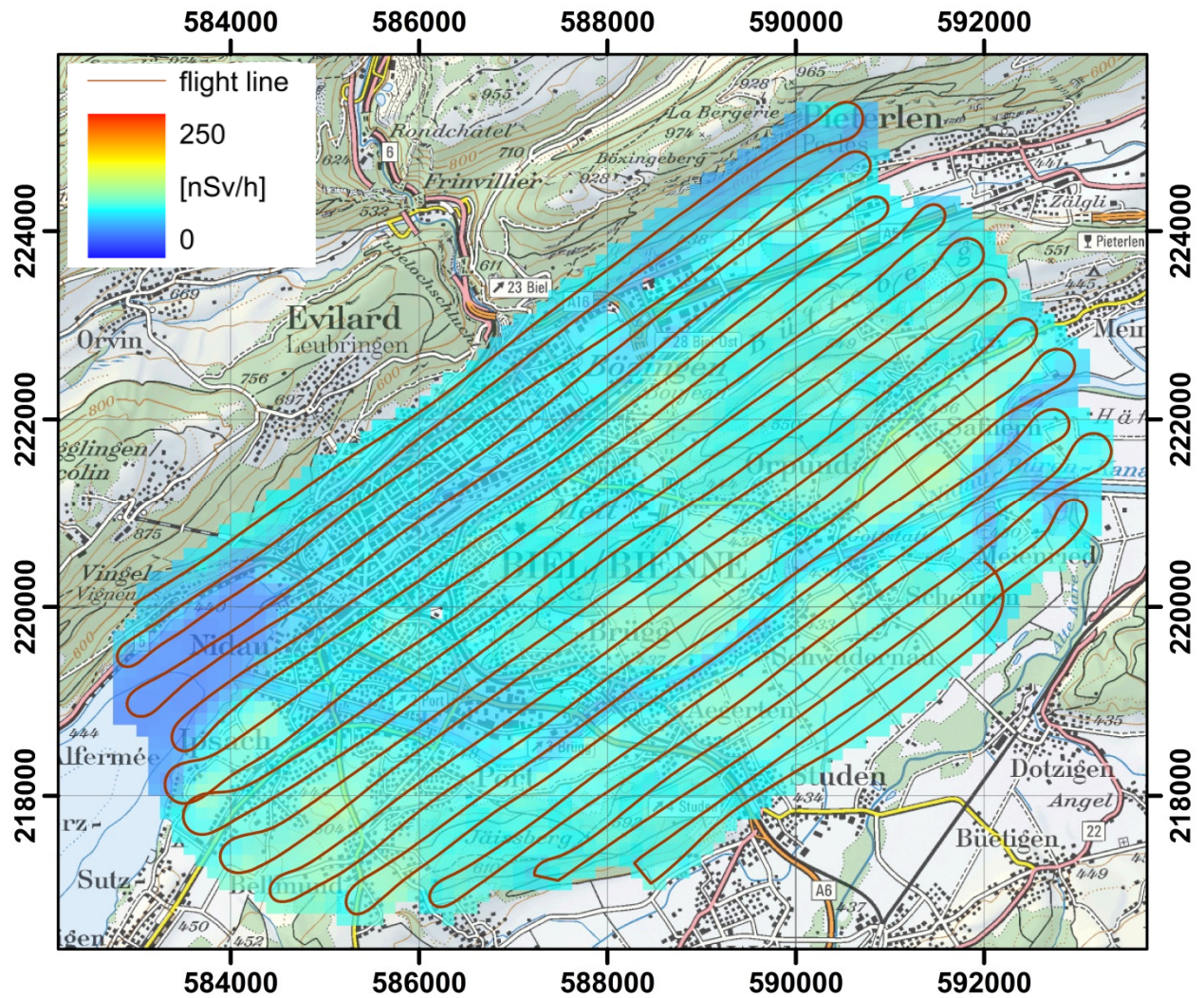


Figure 9: Dose rate over Biel/Bienne city. PK100 © 2013 swisstopo (JD100042)

The dose rate map of the vicinity of Biel/Bienne city (Figure 9) shows normal background values. The attenuation of terrestrial radiation due to the water of Lake Biel yields lower values than observed over dry land.

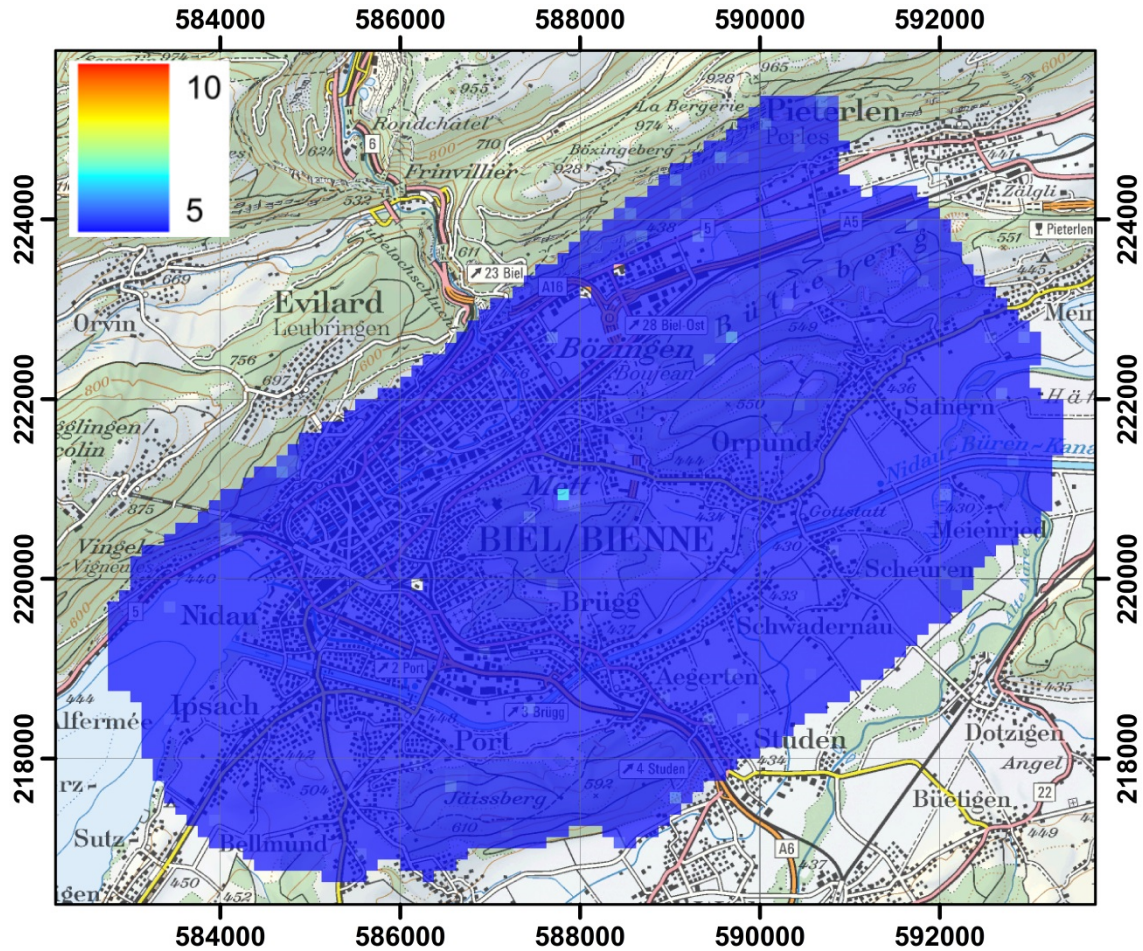


Figure 10: MMGC-ratio over Biel/Bienne city. PK100 © 2013 swisstopo (JD100042)

The map of the MMGC-ratio (Figure 10) shows no significantly elevated values indicating the presence of artificial radionuclides.

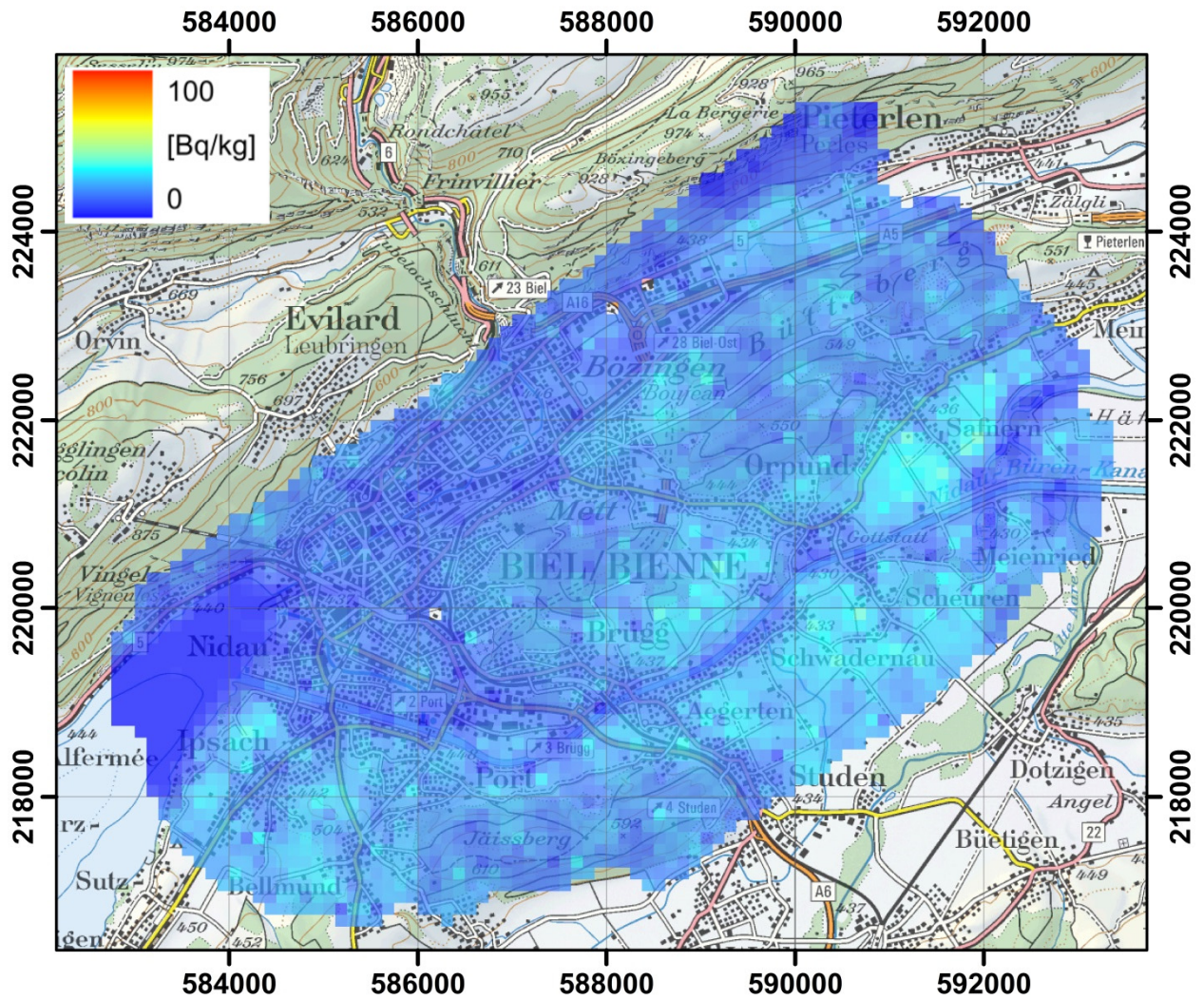


Figure 11: ^{232}Th activity concentration over Biel/Bienne city. PK100 © 2013 swisstopo (JD100042)

The map of the ^{232}Th activity concentration (Figure 11) shows normal background values in the vicinity of Biel/Bienne.

2.4 Thun

The dose rate map of the vicinity of Thun city (Figure 12) shows normal background values. The attenuation of terrestrial radiation due to the water of Lake Thun yields lower values than observed over dry land. The map of the MMGC ratio (Figure 13) yields no indication of the presence of artificial radionuclides. The map of the ^{232}Th activity concentration (Figure 14) shows normal background values.

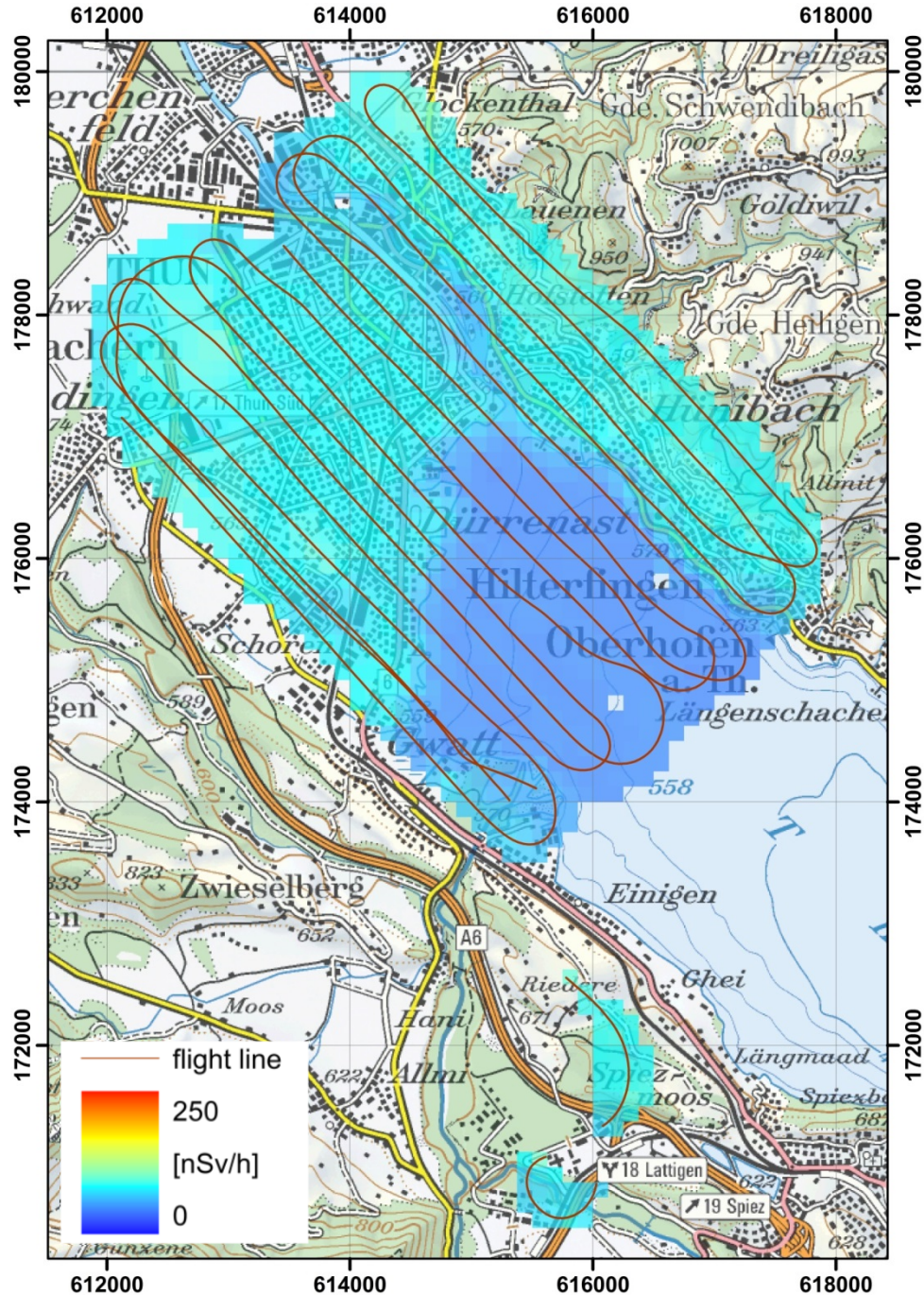


Figure 12: Dose rate over Thun city. PK100 © 2013 swisstopo (JD100042)

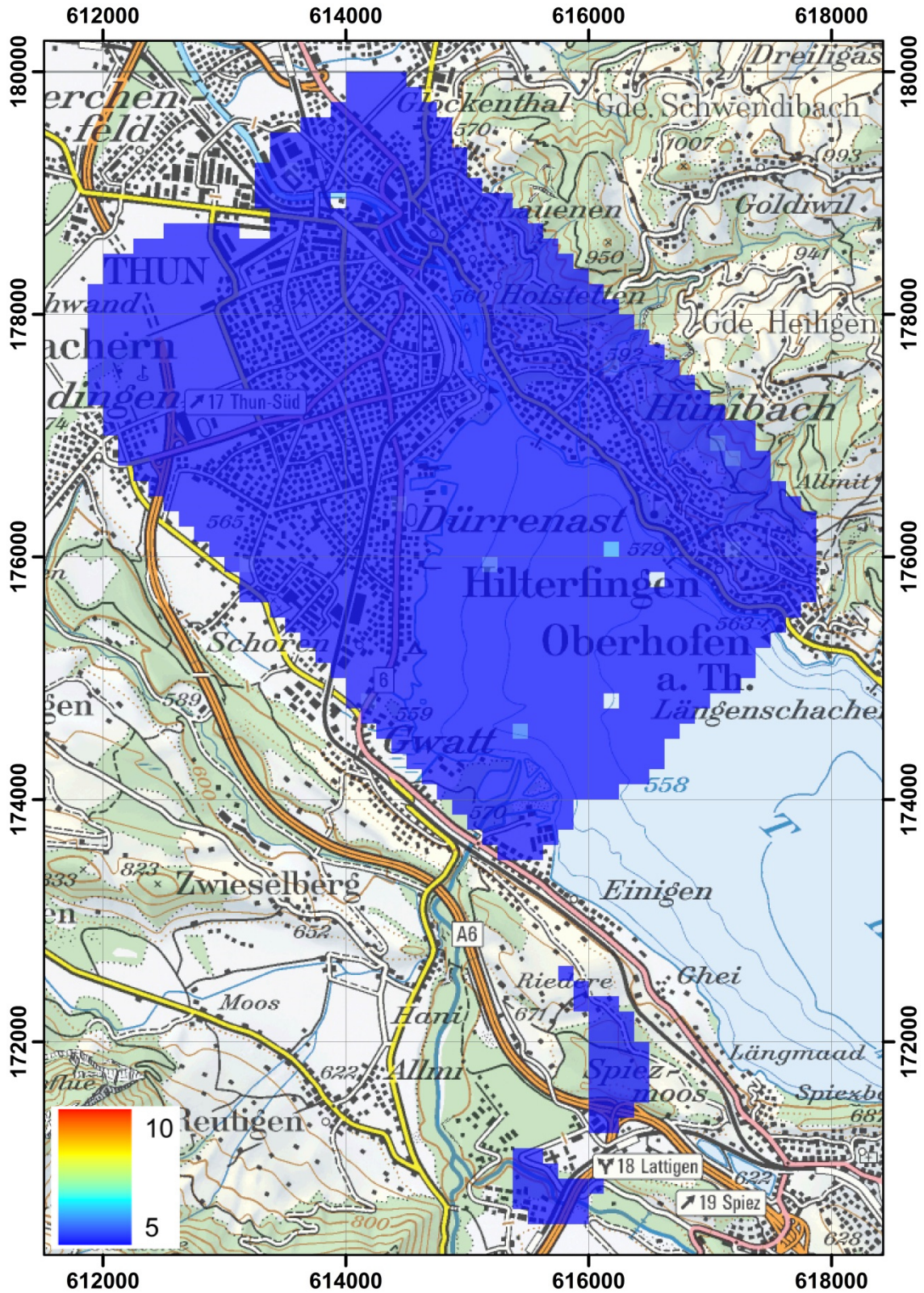


Figure 13: MMGC-ratio over Thun city. PK100 © 2013 swisstopo (JD100042)

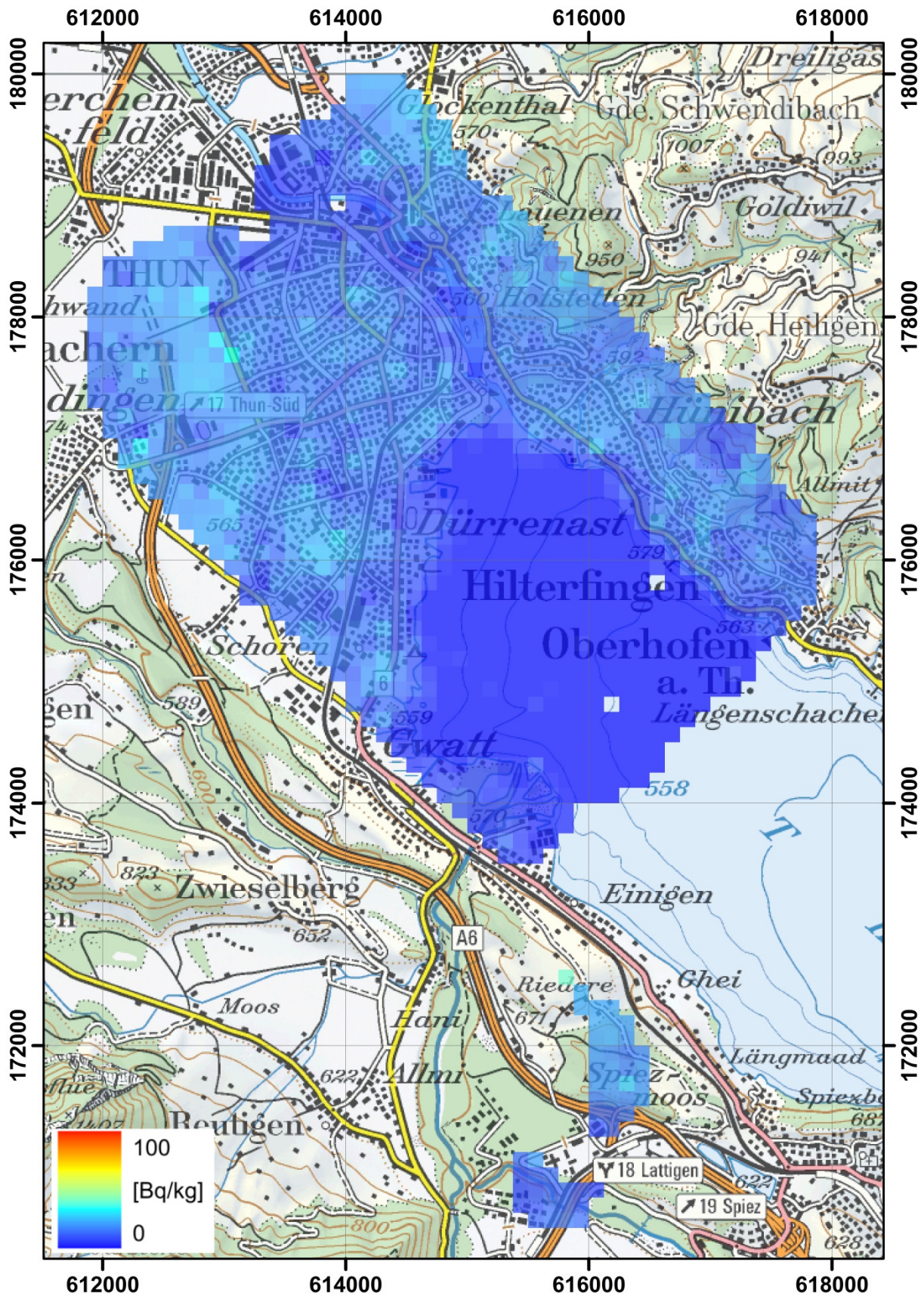


Figure 14: ^{232}Th activity concentration over Thun city. PK100 © 2013 swisstopo (JD100042)

2.5 Kander valley

The maps of the dose rate (Figure 15), of the MMGC-ratio (Figure 16) and of the ^{232}Th activity concentration (Figure 17) measured in the Kander valley show normal background values.

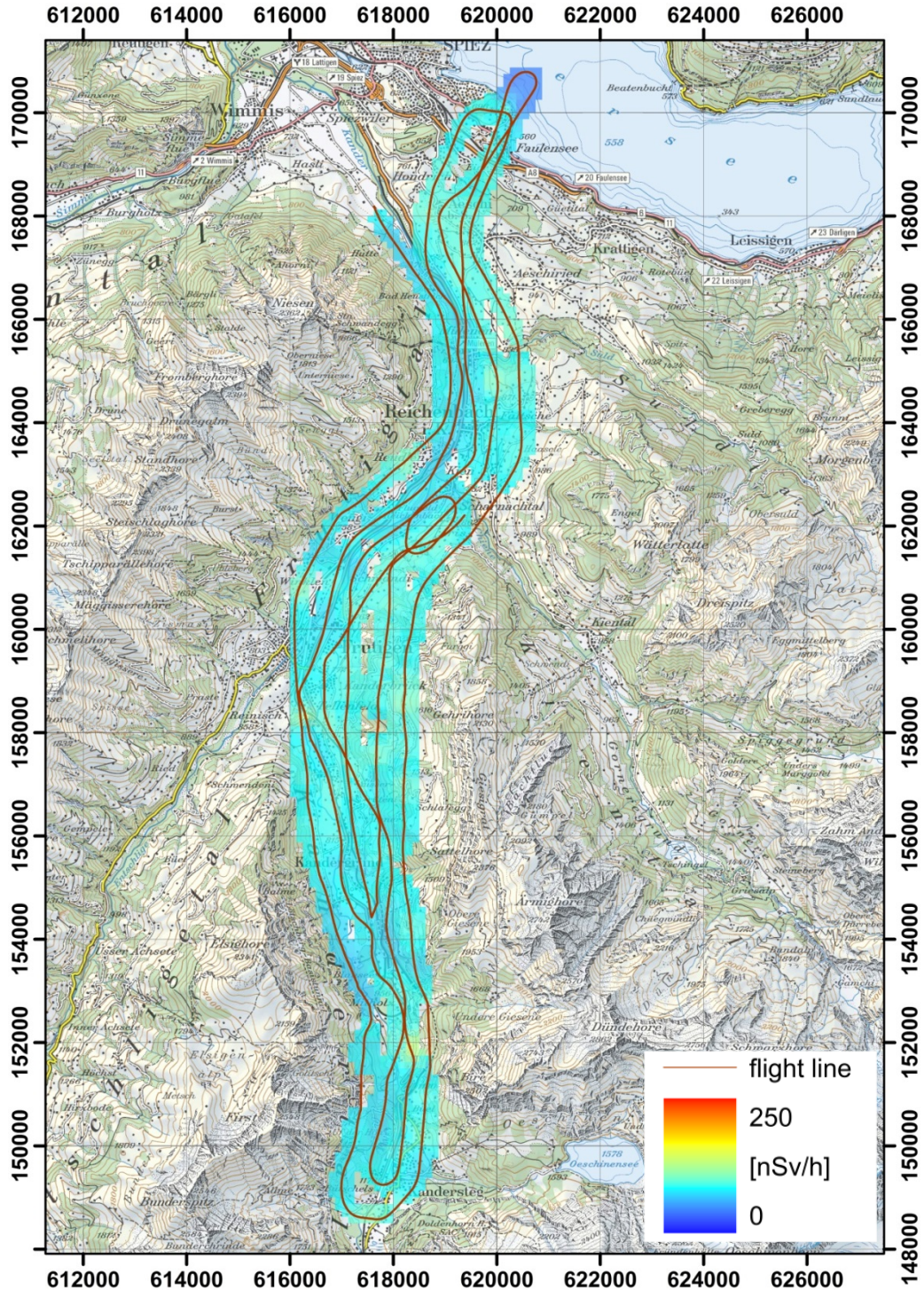


Figure 15: Dose rate in the Kander valley. PK100 © 2013 swisstopo (JD100042)

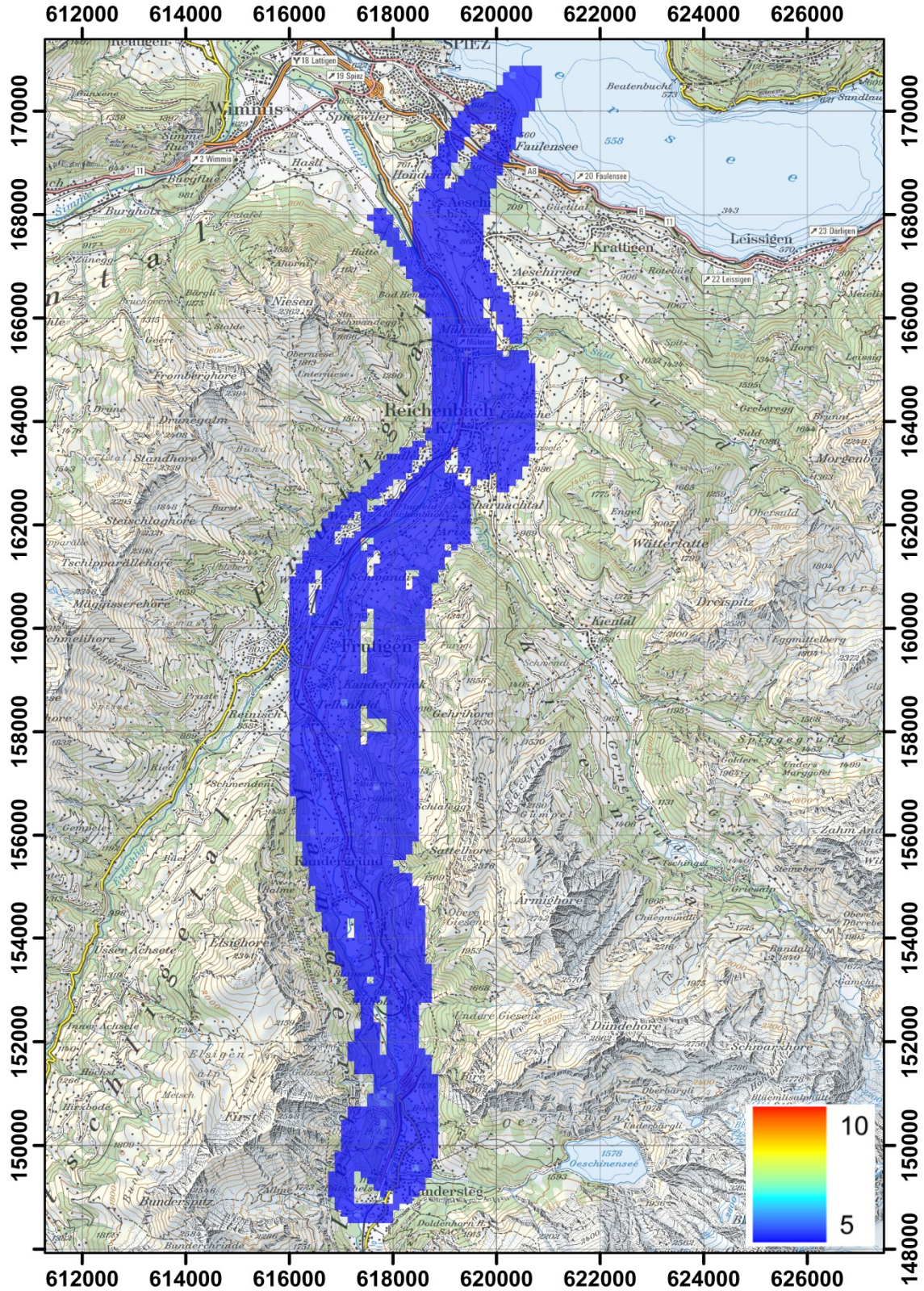


Figure 16: MMGC-ratio in the Kander valley. PK100 © 2013 swisstopo (JD100042)

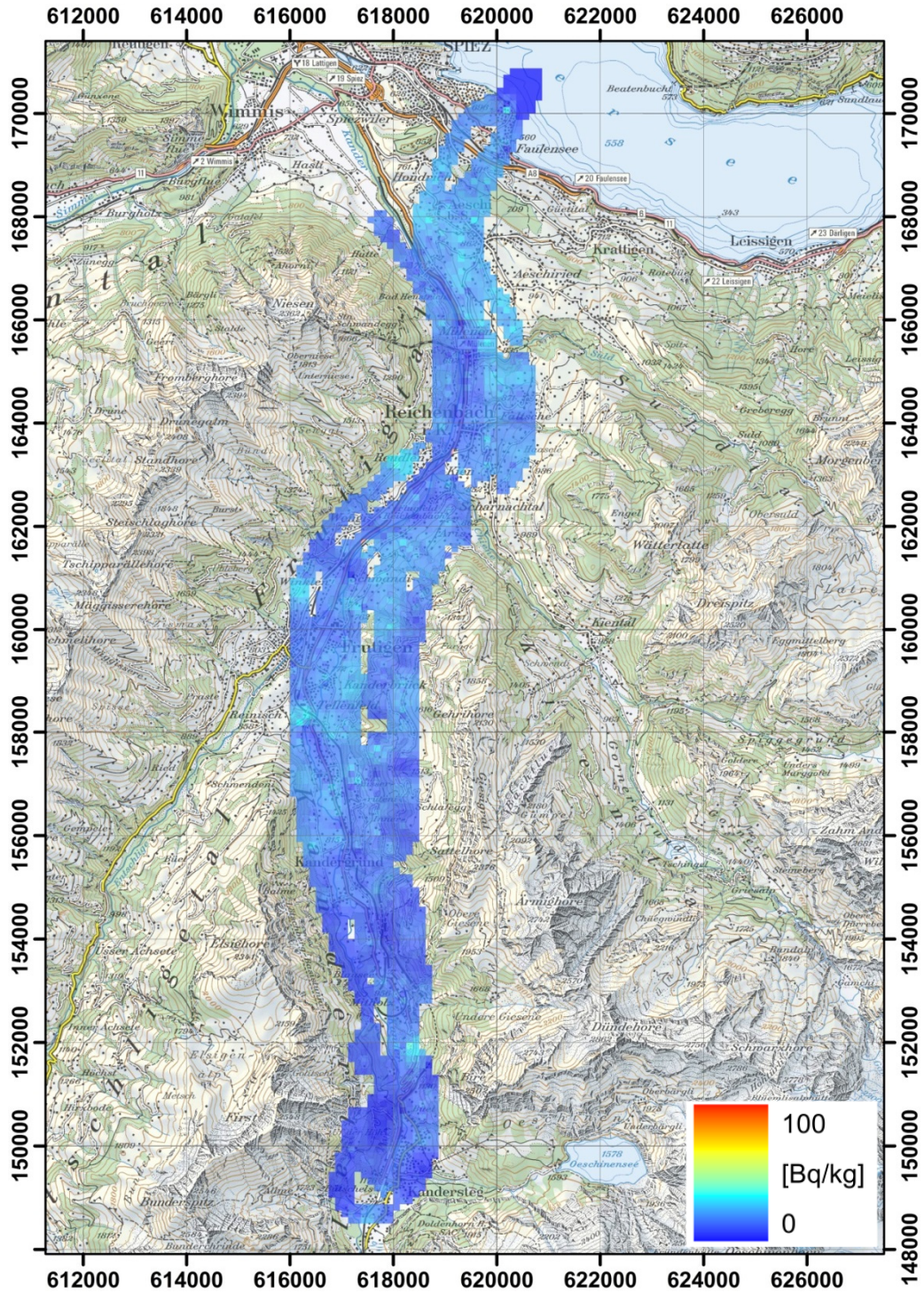


Figure 17: ^{232}Th activity concentration in the Kander valley. PK100 © 2013 swisstopo (JD100042)

2.6 Thun Military training ground

Test of the measuring system and intercomparison measurements with ground instruments were performed on the military training ground near Thun. The ground measurements were performed with a vehicle equipped with gamma spectrometric equipment (Figure 18) operated by KompZen ABC-Kamir, a high pressure ionization chamber operated by ENSI, in-situ gammaspectroscopy and a NaI-based dose rate meter, the latter both operated by Spiez laboratory (Figure 18). The current factory calibration of the vehicle measuring system did not deliver comparable quantities and the respective values are omitted in the comparison.



Figure 18: Vehicle equipped with gamma spectrometric equipment (left) and measurement with high pressure ionisation chamber (right).

The average value of the background dose rate ground measurements agrees well with the average value obtained with airborne gammaspectrometry over the area (Figure 19). Good agreement is also observed in the natural radionuclide content measured with in-situ gammaspectrometry and airborne gammaspectrometry (Figure 20). The error bars depicted in Figure 19 and Figure 20 represent the standard deviation of all data over the measured area. The ^{137}Cs activity concentration at Thun military training ground measured with in-situ gammaspectrometry is with 7 ± 1 Bq/kg well below the detection limit of the airborne gammaspectrometry.

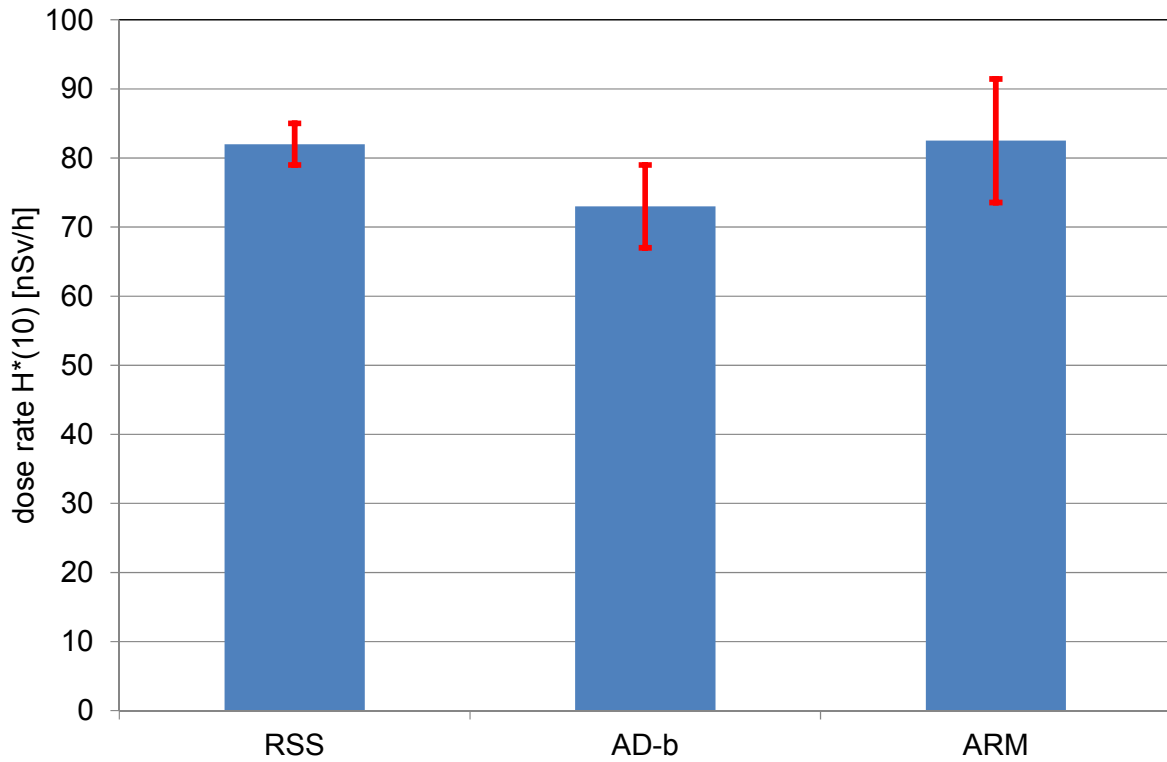


Figure 19: Background dose rate at Thun military ground measured with a high pressure ionization chamber (RSS), NaI-based dose meter (AD-b) and airborne gamma spectroscopy (ARM).

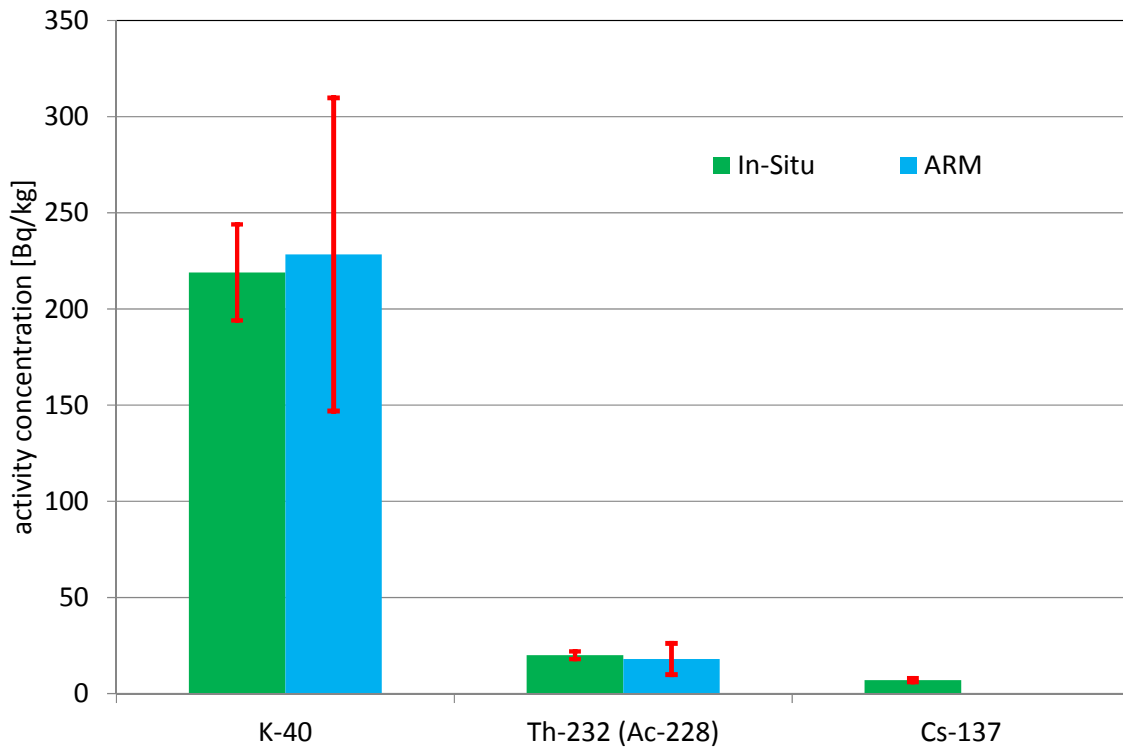


Figure 20: Activity concentrations of the radionuclides ^{40}K , ^{232}Th and ^{137}Cs measured with in-situ gamma spectrometry on the ground and airborne gamma spectrometry at Thun military ground.

A ^{137}Cs -Source (4.5 GBq) and a ^{60}Co -Source (750 MBq) were placed consecutively at two positions on a meadow and in a copse. Figure 21 shows the two source positions, the route of the gamma spectrometric vehicle to locate the ^{60}Co source at the meadow position and the dose rate measured with the vehicle.

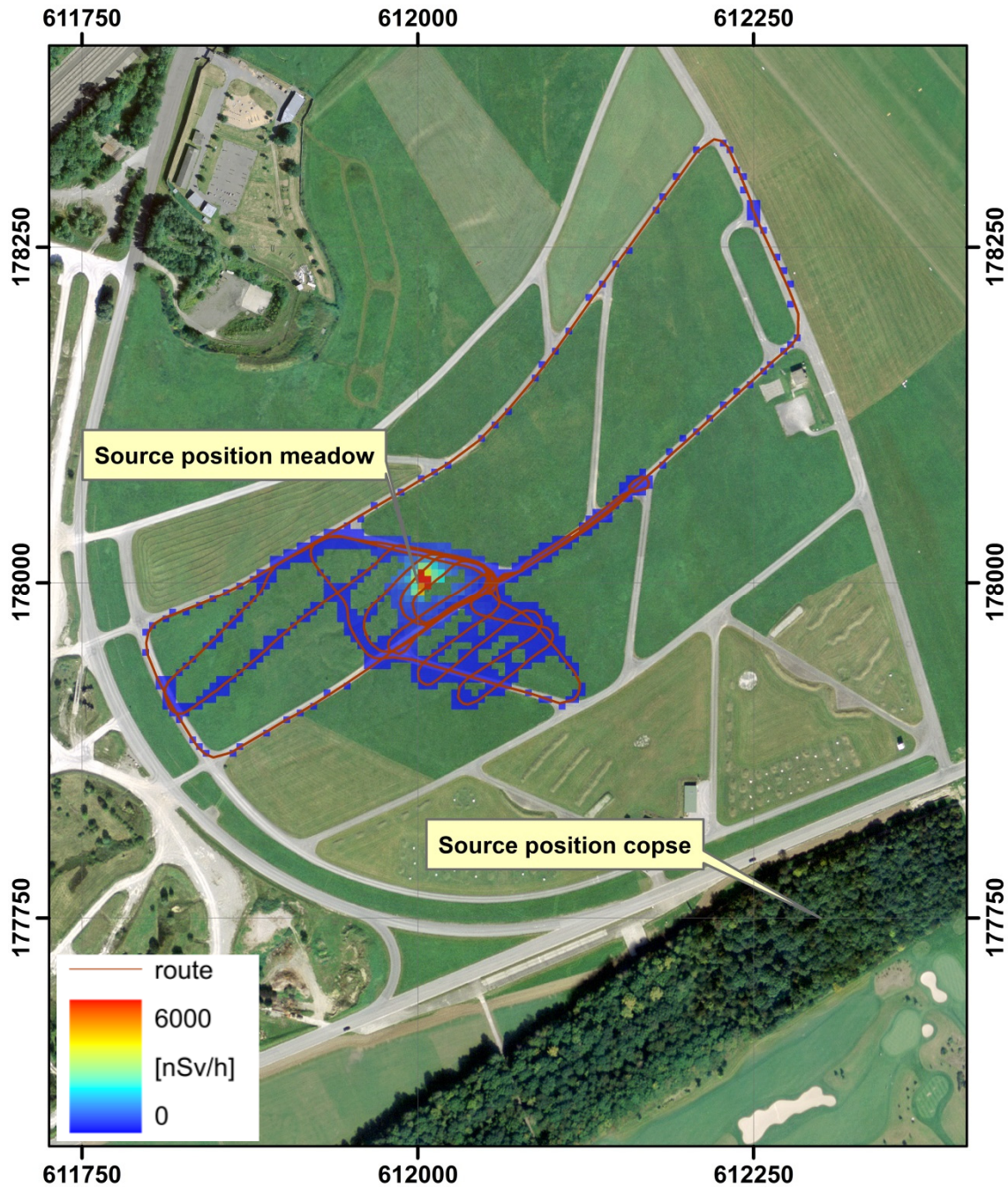


Figure 21: Aerial view of the Thun military ground, route of the gamma-spectrometry vehicle and measured dose rate. swissimage 25 © 2013 swisstopo (JD100042)

The position of the sources was detected both with airborne and vehicle gamma spectroscopy. An estimate of source activity could only be determined with the airborne system. Figure 22 shows a comparison of the estimated activity derived from the measured spectra to the true activity of the placed sources. The error bars included in Figure 22 represent the combined extended measurement uncertainty with an expansion factor $k=2$. The measured activities agree within the specified uncertainties. Compared to the specified source activity, the measurement overestimates the activity up to a factor of 1.7.

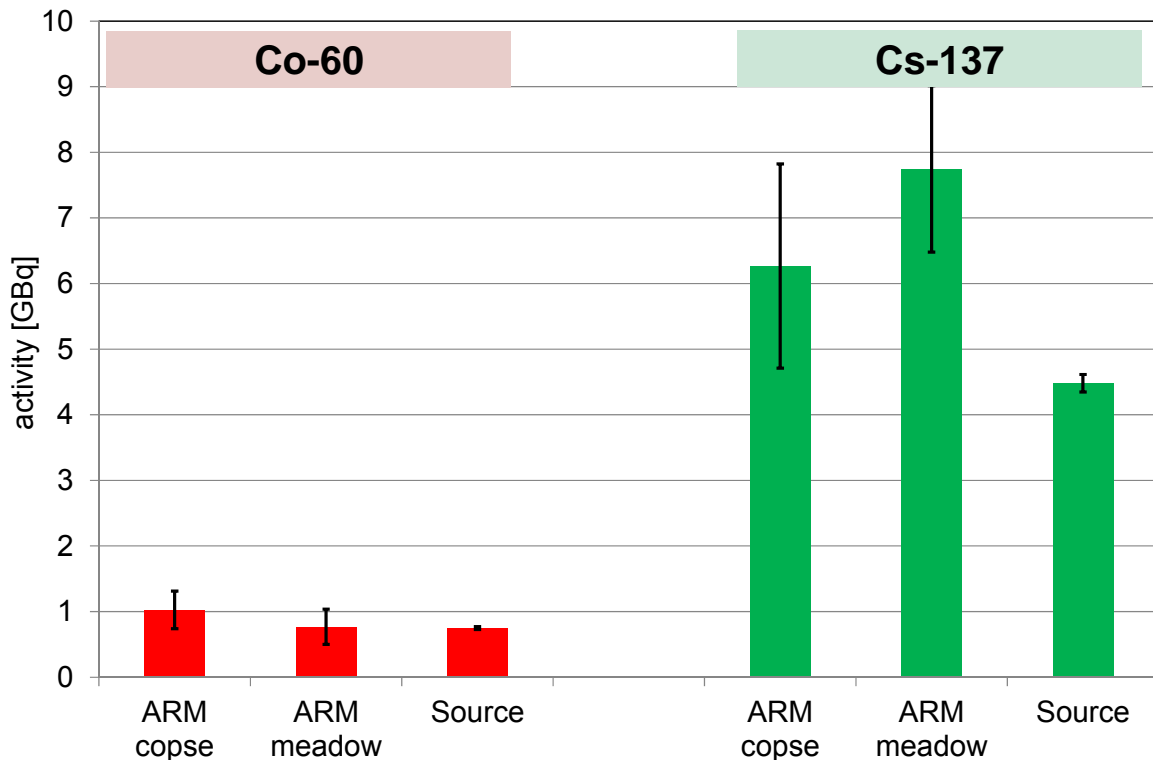


Figure 22: Comparison of the estimated source activity determined with airborne gamma spectrometry (ARM) at two source positions to the real source activity

The helicopter hovered over the meadow source positions in different heights to check on the appropriate correction factors. The measurement started with the largest height to prevent the strong signal of especially the ^{60}Co source to impair the automatic spectrum stabilization using the ^{40}K -signal. Both measurements over the ^{60}Co and ^{137}Cs sources show a distinct height dependence of the estimated source activity (Figure 23 and Figure 24). The source activity is estimated using two steps. First, the measured signal is extrapolated with an exponential function from the actual height above ground to the reference height of 100 m. In a second step a calibration factor is applied to the extrapolated value. The routine used for extrapolating to the reference height is mainly used and optimized for mapping extended contaminated areas. For point sources, an additional correction is needed taking into account the diminution of the radiation field proportional to the square of the source distance.

Due to the results of the presented data, a more flexible algorithm has been implemented in a revision of the evaluation software, taking into account the purpose of

the flight (e.g. mapping or source search). Figure 25 and Figure 26 show the reduced altitude dependence with the revised data evaluation.

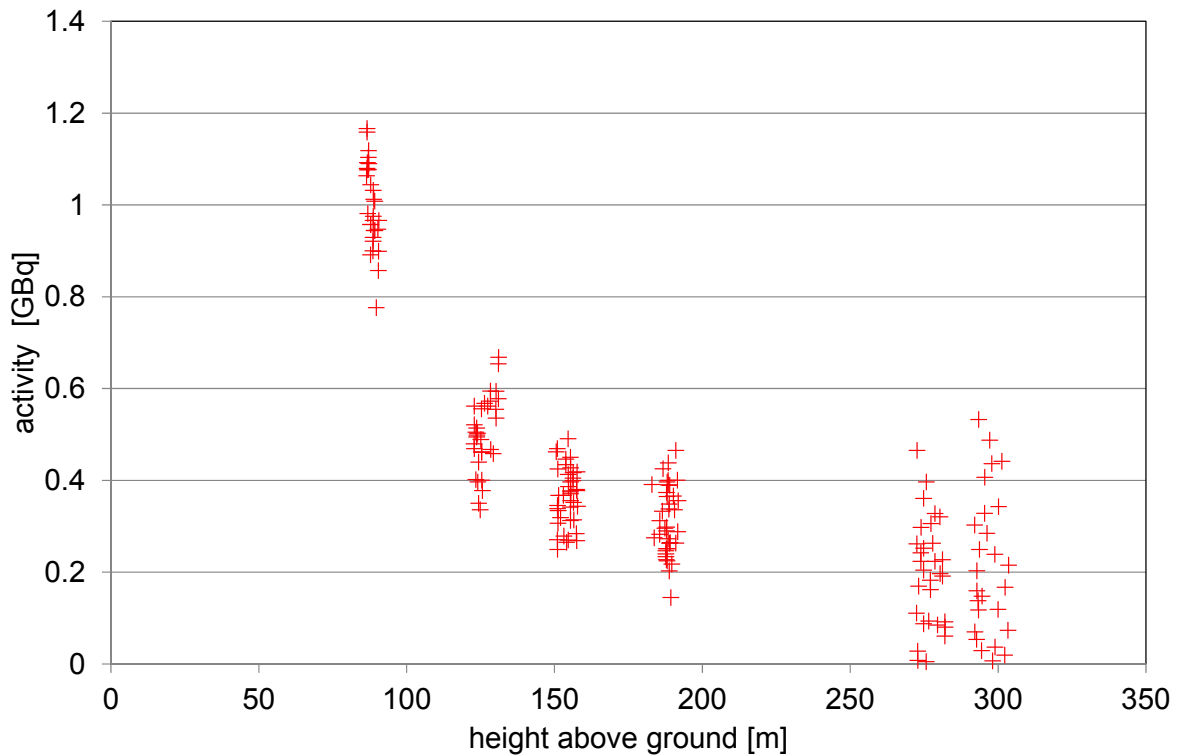


Figure 23: Activity of a ^{60}Co source determined with airborne gamma spectrometry at different heights above ground.

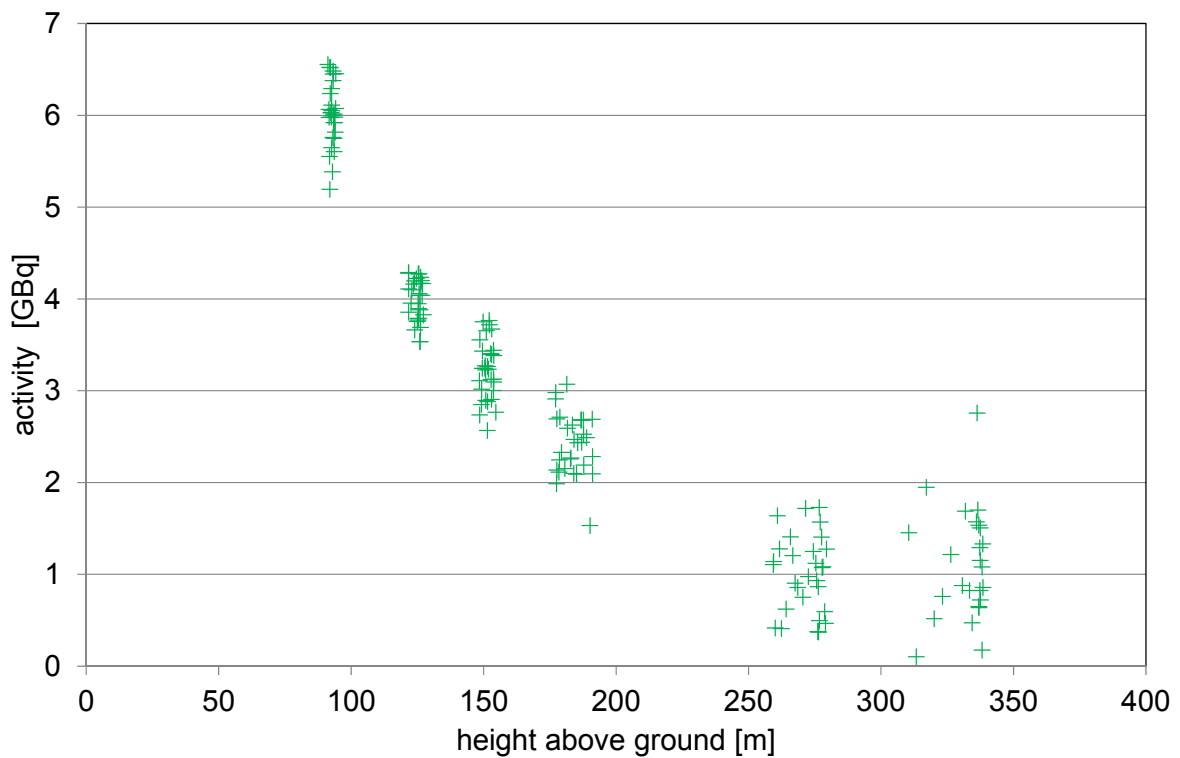


Figure 24: Activity of a ^{137}Cs source determined with airborne gamma spectrometry at different heights above ground.

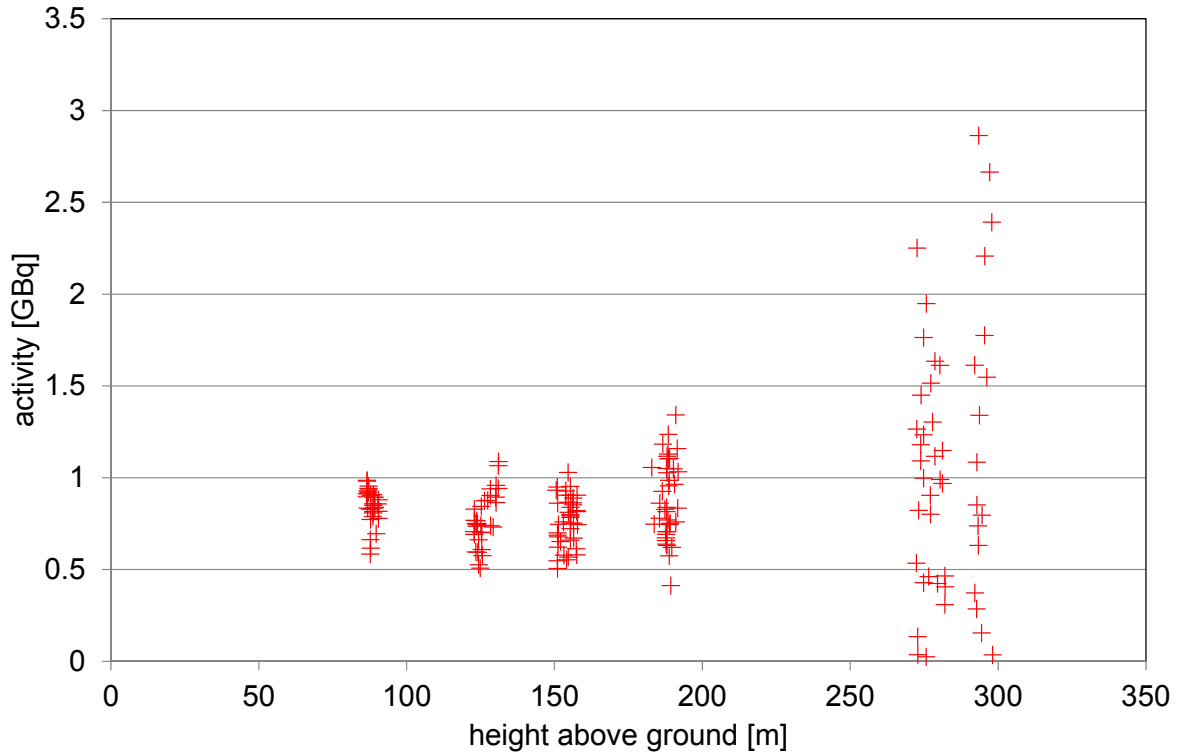


Figure 25: Activity of a ^{60}Co source determined with airborne gamma spectrometry at different heights above ground.

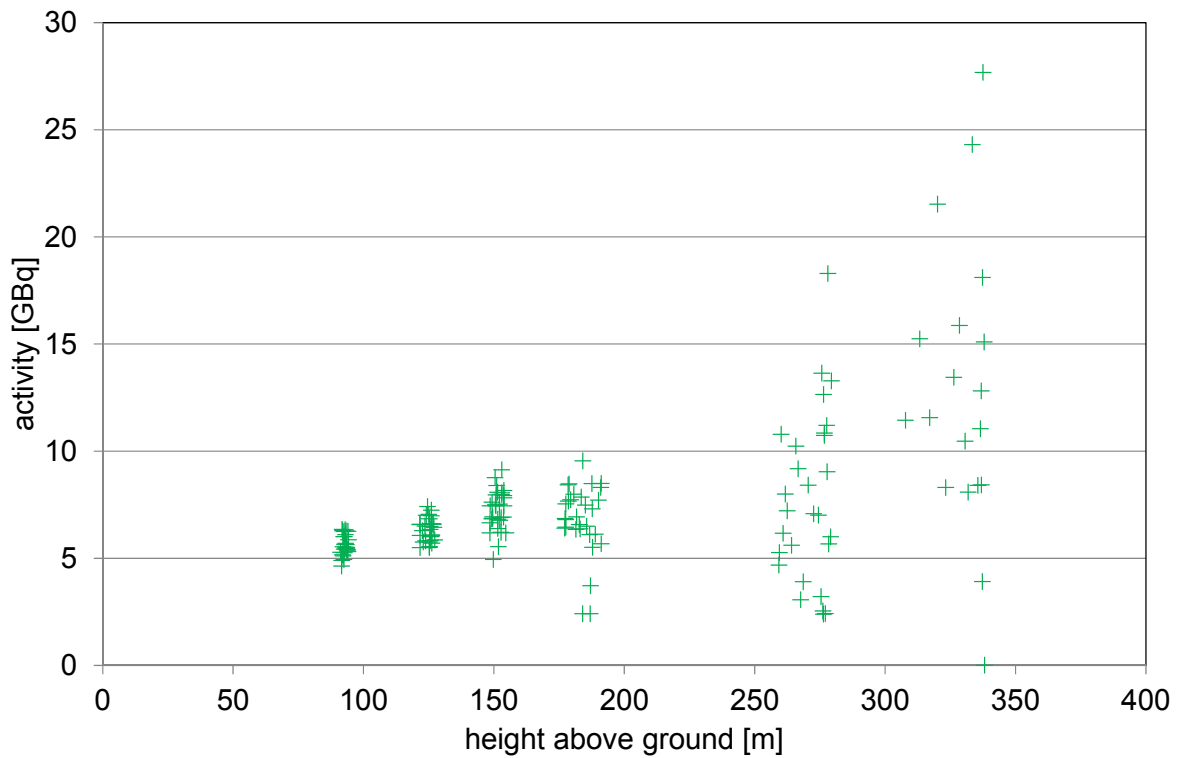


Figure 26: Activity of a ^{137}Cs source determined with airborne gamma spectrometry at different heights above ground.

2.7 Flight Berne – Zurich

The data of airborne radiological measurements can be used as input for the generation of baseline radiological maps (Rybach et al., 1996). Thus, a target of the annual airborne gamma spectrometry exercises is the measurement of areas not yet covered by the flights. In 2013, a flight from Berne to Zurich (Figure 27) was applied in this context. The terrestrial dose rate (Figure 28) showed typical background values around 50 nSv/h with significantly lower dose rates over larger bodies of water.

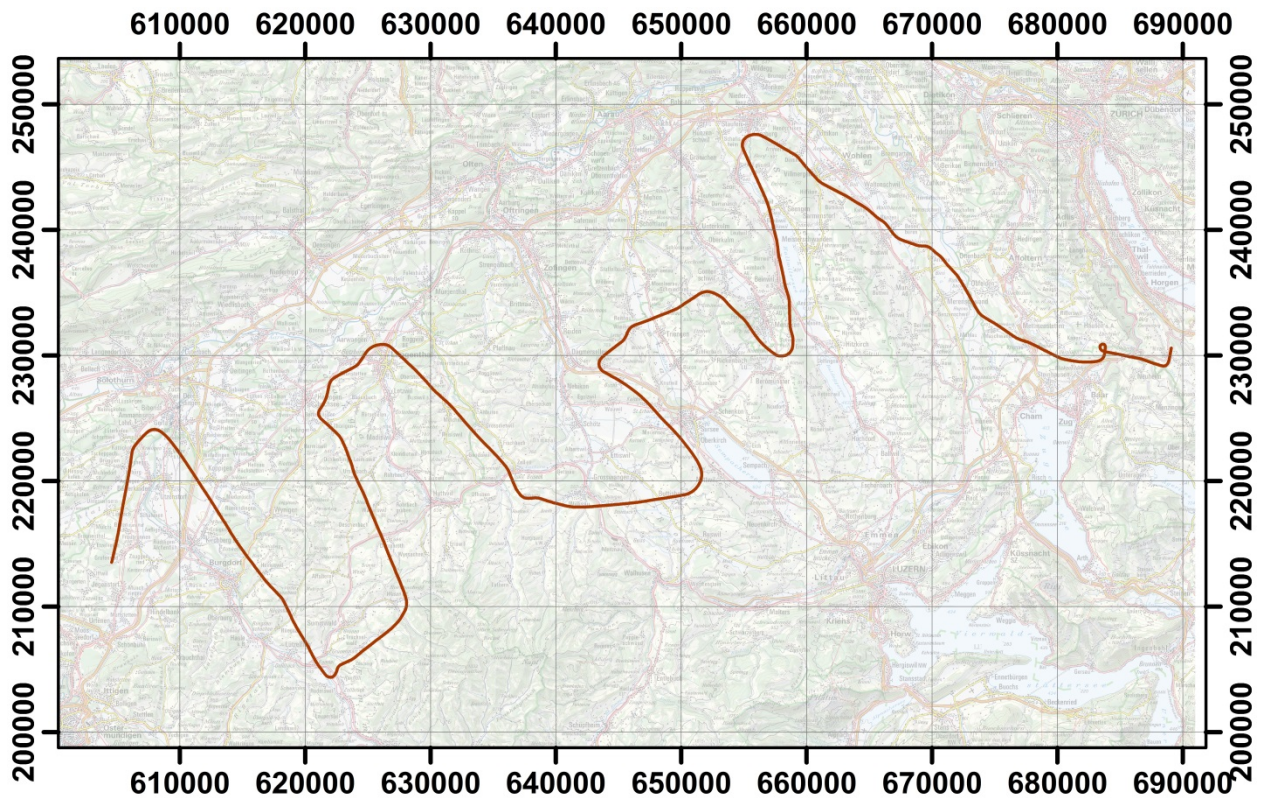


Figure 27: Flight line of the measuring flight from Berne to Zurich. PK200 © 2013 swisstopo (JD100042)

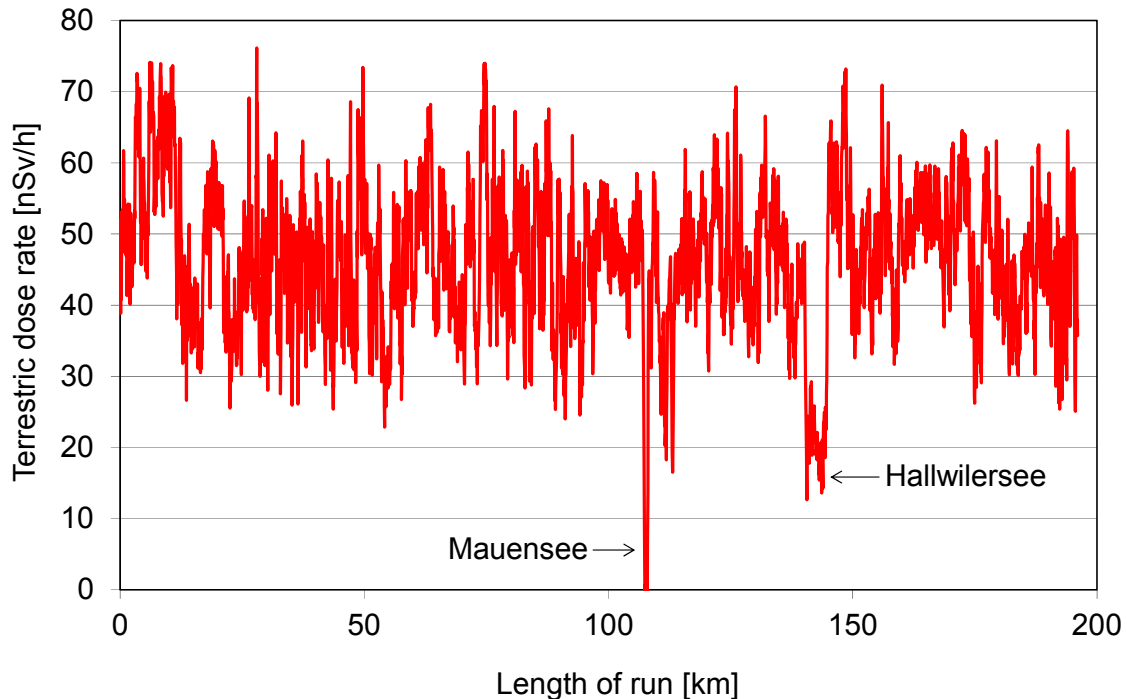


Figure 28: Terrestrial dose rate along the profile from Berne to Zurich.

3 CONCLUSIONS

The measurement over the nuclear power plants Gösigen (KKG) and Mühleberg (KKM), following a bi-annual routine showed no artificial radionuclides outside of the plant premises. As in previous years, the distinction between pressurized and boiling water reactor is clearly identified from the photon spectra.

Further measurement areas showed typical background readings.

Intercomparison between airborne and ground measurements showed good agreement.

Test flights over a military training ground led to an improvement of the algorithm for estimating point source activities.

4 LITERATURE

Schwarz, G. F.: Methodische Entwicklungen zur Aerogammaspektrometrie. Beiträge zur Geologie der Schweiz, Geophysik Nr. 23, Schweizerische Geophysikalische Kommission, 1991.

Rybach, L., Schwarz, G. F. and Medici, F.: Construction of radioelement and dose-rate baseline maps by combining ground and airborne radiometric data. IAEA-Tecd-980, 33–44, Vienna, 1996

Bucher, B.: Methodische Weiterentwicklungen in der Aeroradiometrie. Dissertation Nr. 13973, ETH Zürich, 2001.

5 PREVIOUS REPORTS

Schwarz, G. F., Klingelé, E. E., Rybach, L.: Aeroradiometrische Messungen in der Umgebung der schweizerischen Kernanlagen. Bericht für das Jahr 1989 zuhanden der Hauptabteilung für die Sicherheit der Kernanlagen (HSK). Interner Bericht, Institut für Geophysik, ETH Zürich, 1990.

Schwarz, G. F., Klingelé, E. E., Rybach, L.: Aeroradiometrische Messungen in der Umgebung der schweizerischen Kernanlagen. Bericht für das Jahr 1990 zuhanden der Hauptabteilung für die Sicherheit der Kernanlagen (HSK). Interner Bericht, Institut für Geophysik, ETH Zürich, 1991.

Schwarz, G. F., Klingelé, E. E., Rybach, L.: Aeroradiometrische Messungen in der Umgebung der schweizerischen Kernanlagen. Bericht für das Jahr 1991 zuhanden der Hauptabteilung für die Sicherheit der Kernanlagen (HSK). Interner Bericht, Institut für Geophysik, ETH Zürich, 1992.

Schwarz, G. F., Klingelé, E. E., Rybach, L.: Aeroradiometrische Messungen in der Umgebung der schweizerischen Kernanlagen. Bericht für das Jahr 1992 zuhanden der Hauptabteilung für die Sicherheit der Kernanlagen (HSK). Interner Bericht, Institut für Geophysik, ETH Zürich, 1993.

Schwarz, G. F., Klingelé, E. E., Rybach, L.: Aeroradiometrische Messungen in der Umgebung der schweizerischen Kernanlagen. Bericht für das Jahr 1993 zuhanden der Hauptabteilung für die Sicherheit der Kernanlagen (HSK). Interner Bericht, Institut für Geophysik, ETH Zürich, 1994.

Schwarz, G. F., Rybach, L.: Aeroradiometrische Messungen im Rahmen der Übung ARM94. Bericht für das Jahr 1994 zuhanden der Fachgruppe Aeroradiometrie (FAR). Interner Bericht, Institut für Geophysik, ETH Zürich, 1995.

Schwarz, G. F., Rybach, L.: Aeroradiometrische Messungen im Rahmen der Übung ARM95. Bericht für das Jahr 1995 zuhanden der Fachgruppe Aeroradiometrie (FAR). Interner Bericht, Institut für Geophysik, ETH Zürich, 1996.

Schwarz, G. F., Rybach, L., Bärlocher, C.: Aeroradiometrische Messungen im Rahmen der Übung ARM96. Bericht für das Jahr 1996 zuhanden der Fachgruppe Aeroradiometrie (FAR). Interner Bericht, Institut für Geophysik, ETH Zürich, 1997.

Bucher, B., Rybach, L., Schwarz, G., Bärlocher, C.: Aeroradiometrische Messungen im Rahmen der Übung ARM97. Bericht für das Jahr 1997 zuhanden der Fachgruppe Aeroradiometrie (FAR). Interner Bericht, Institut für Geophysik, ETH Zürich, 1998.

Bucher, B., Rybach, L., Schwarz, G., Bärlocher, C.: Aeroradiometrische Messungen im Rahmen der Übung ARM98. Bericht für das Jahr 1998 zuhanden der Fachgruppe Aeroradiometrie (FAR). Interner Bericht, Institut für Geophysik, ETH Zürich, 1999.

Bucher, B., Rybach, L., Schwarz, G., Bärlocher, C.: Aeroradiometrische Messungen im Rahmen der Übung ARM99. Bericht für das Jahr 1999 zuhanden der Fachgruppe Aeroradiometrie (FAR). Interner Bericht, Institut für Geophysik, ETH Zürich, 2000.

Bucher, B., Rybach, L., Schwarz, G., Bärlocher, C.: Aeroradiometrische Messungen im Rahmen der Übung ARM00. Bericht für das Jahr 2000 zuhanden der Fachgruppe Aeroradiometrie (FAR). Interner Bericht, Institut für Geophysik, ETH Zürich, 2001.

Bucher, B., Rybach, L., Schwarz, G., Bärlocher, C.: Aeroradiometrische Messungen im Rahmen der Übung ARM01. Bericht für das Jahr 2001 zuhanden der Fachgruppe Aeroradiometrie (FAR). Interner Bericht, Paul Scherrer Institut, Villigen, Schweiz, 2002.

Bucher, B., Rybach, L., Schwarz, G., Bärlocher, C.: Aeroradiometrische Messungen im Rahmen der Übung ARM02. Bericht für das Jahr 2002 zuhanden der Fachgruppe Aeroradiometrie (FAR). Interner Bericht, Paul Scherrer Institut, Villigen, Schweiz, 2003.

Bucher, B., Rybach, L., Schwarz, G.: Aeroradiometrische Messungen im Rahmen der Übung ARM03. PSI-Bericht 04-14, ISSN 1019-0643, Paul Scherrer Institut, Villigen, Schweiz, 2004.

Bucher, B., Butterweck, G., Rybach, L., Schwarz, G.: Aeroradiometrische Messungen im Rahmen der Übung ARM04. PSI-Bericht 05-10, ISSN 1019-0643, Paul Scherrer Institut, Villigen, Schweiz, 2005.

Bucher, B., Butterweck, G., Rybach, L., Schwarz, G.: Aeroradiometrische Messungen im Rahmen der Übung ARM05. PSI-Bericht 06-06, ISSN 1019-0643, Paul Scherrer Institut, Villigen, Schweiz, 2006.

Bucher, B., Butterweck, G., Rybach, L., Schwarz, G.: Aeroradiometrische Messungen im Rahmen der Übung ARM06. PSI-Bericht 07-02, ISSN 1019-0643, Paul Scherrer Institut, Villigen, Schweiz, 2007.

Bucher, B., Guillot, L., Strobl, C., Butterweck, G., Gutierrez, S., Thomas, M., Hohmann, C., Krol, I., Rybach, L., Schwarz, G.: International Intercomparison Exercise of Airborne Gamaspectrometric Systems of Germany, France and Switzerland in the Framework of the Swiss Exercise ARM07. PSI-Bericht Nr. 09-07, ISSN 1019-0643, Paul Scherrer Institut, Villigen, Schweiz, 2009.

Bucher, B., Butterweck, G., Rybach, L., Schwarz, G.: Aeroradiometrische Messungen im Rahmen der Übung ARM08. PSI-Bericht Nr. 09-02, ISSN 1019-0643, Paul Scherrer Institut, Villigen, Schweiz, 2009.

Bucher, B., Butterweck, G., Rybach, L., Schwarz, G., Strobl, C.: Aeroradiometrische Messungen im Rahmen der Übung ARM09. PSI-Bericht Nr. 10-01, ISSN 1019-0643, Paul Scherrer Institut, Villigen, Schweiz, 2010.

Bucher, B., Butterweck, G., Rybach, L., Schwarz, G., Mayer, S.: Aeroradiometrische Messungen im Rahmen der Übung ARM10. PSI-Bericht Nr. 11-02, ISSN 1019-0643, Paul Scherrer Institut, Villigen, Schweiz, 2011.

Bucher, B., Butterweck, G., Rybach, L., Schwarz, G., Mayer, S.: Aeroradiometric Measurements in the Framework of the Swiss Exercise ARM11. PSI-Report No. 12-04, ISSN 1019-0643, Paul Scherrer Institut, Villigen, Switzerland, 2012.

Butterweck, G., Bucher, B., Rybach, L., Schwarz, G., Hödlmoser, H., Mayer, S., Danzi, C., Scharding, G.: Aeroradiometric Measurements in the Framework of the Swiss Exercise ARM12. PSI-Report No. 13-01, ISSN 1019-0643, Paul Scherrer Institut, Villigen, Switzerland, 2013.

The reports since 1994 can be found and downloaded from the FAR website <http://www.far.ensi.ch>.

6 EVALUATION PARAMETER FILES

The parameter files used for the evaluation of raw data during this exercise are listed below to improve the traceability of the presented results.

6.1 DefinitionFile_Processing.txt

This file defines the parameters used for the gridding of evaluated parameters.

```
----- Start of file -----
Definition file Swiss MGS32
"Windows"
10
Total 401. 2997. 0. 0
K-40 1369. 1558. 1460. 1
U-238 1664. 1853. 1765. 1
Th-232 2407. 2797. 2615. 1
Cs-137 600. 720. 660. 2
Co-60 1100. 1400. 0. 2
MMGC1 400. 1400. 0. 0
MMGC2 1400. 2997. 0. 0
LOW 40. 720. 0. 0
MID 720. 2997. 0. 0
"Ratios"
3
MMGCVerhältnis MMGC1 MMGC2 Ratio_MMGC
LOWHigh LOW MMGC2 RatioLowHigh
LowMid LOW MID RatioLowMid
"Conversion factors Activity to Dose Rate"
8
Total 0 NoCalibration " " 0
AD_K-40 0.044 DHSR "nSv/h" 1
AD_U-238 0.55 DHSR "nSv/h" 1
AD_Th-232 0.77 DHSR "nSv/h" 1
AD_Cs-137 0.2 DHSR "nSv/h" 2
Co-60 0 NoCalibration " " 0
MMGC1 0 NoCalibration " " 0
MMGC2 0 NoCalibration " " 0
"Typ des Darstellungsgrenzwertes"
1
Nachweistyp 0
"counts of spectra to stack"
1
Counts 1
"Auszugebende Werte"
30
```

```

"DHSR TOT      ", "DHSR_TOT", "nSv/h      ", 0.00, 250.00
"AP_Co-60     ", "AP_Co-60", "MBq      ", 0.00, 150.00
"AP_Cs-137    ", "AP_Cs-137", "MBq      ", 0.00, 40.00
"Terr. DL     ", "DHSR_TOT", "nSv/h      ", 0.00, 250.00
"CR_Caesium   ", "CR_Cs-137", "cps      ", 20.00, 120.00
"CR_Cobalt    ", "CR_Co-60", "cps      ", 0.00, 100.00
"Low-HighRatio", "RatioLowHigh", "%      ", 0.00, 1000.00
"Low-MidRatio ", "RatioLowMid", "%      ", 0.00, 1000.00
"Total_CR_corr", "NR_Total", "cps      ", 200.00, 1200.00
"K-40         ", "AD_K-40", "Bq/kg     ", 0.00, 1000.00
"U-238        ", "AD_U-238", "Bq/kg     ", 0.00, 120.00
"Th-232       ", "AD_Th-232", "Bq/kg     ", 0.00, 120.00
"Cs-137       ", "AD_Cs-137", "Bq/kg     ", 0.00, 240.00
"Cobalt_CR    ", "NR_Co-60", "cps      ", 0.00, 120.00
"Nat.Terr.DL  ", "DHSR_NAT", "nSv/h      ", 0.00, 250.00
"Künst.DL    ", "DHSR_ANT", "nSv/h      ", 0.00, 250.00
"MMGC_Ratio   ", "MMGC_Ratio", "%      ", 400, 600.00
"Cosmic DL    ", "DHSR_COS", "nSv/h      ", 20.00, 60.00
"Cosmic       ", "CR_COS", "cps      ", 000.00, 400.00
"Radar        ", "PH", "m      ", 0.00, 300.00
"ODL          ", "DHSR", "nSv/h      ", 0.00, 250
"AD_UT_K-40   ", "AD_UT_K-40", "Bq/kg     ", 0.00, 200
"CR_MMGC2     ", "CR_MMGC2", "cps      ", 0.00, 1000.00
"AD_UT_Th-232", "AD_UT_Th-232", "Bq/kg     ", 0.00, 40
"AD_UT_Cs-137", "AD_UT_Cs-137", "Bq/kg     ", 0.00, 20
"Err_Co-60    ", "NR_UT_Co-60", "cps      ", 0.00, 40
"Nachweis_Cs-137", "CR_LD_Cs-137", "cps      ", 0.00, 100.00
"Nachweis_Co-60", "CR_LD_Co-60", "cps      ", 0.00, 100.00
"Cs-137 beta=0", "AA_Cs-137", "Bq/m2     ", 0.00, 20000.00
"AA_UT_Cs-137", "AA_UT_Cs-137", "Bq/m2     ", 0.00, 20

```

----- End of file -----

6.2 DefinitionFile_DetC.txt

This file defines the parameters used for the derivation of dose rates and activity concentrations from the raw spectra. The current file is customized for the 16-litre-detector purchased from Exploranium in the year 2007. This detector was used in all measurements since the year 2007.

----- Start of file -----

```

Definition file System
"Koordinaten"
WGS84
"Non-linearity"
4
a0 0.6966
a1 0.08423
a2 -0.0000032807
a3 0.00000000042937
"Recorder old RDT-Files"
8

```


Radar 0.00 -61.00
 Baro 0.74 457.14
 Cosm 0.00 1.00
 Dead 5.00 0.00
 Time 0.00 1.00
 Temp 0.00 1.00
 Pitch 0.00 76.20
 Roll 0.00 90.91

"Background/Cosmic"

10

Total	98.1000	1.041	0.032
K-40	12.100	0.050	0.004
U-238	2.700	0.043	0.002
Th-232	3.400	0.044	0.001
Cs-137	15.500	0.102	0.005
Co-60	13.900	0.100	0.004
MMGC1	79.540	0.771	0.019
MMGC2	18.500	0.270	0.007
LOW	0.	0.	0.
MID	0.	0.	0.

"Stripping Coefficients"

10

1.000	0.000	0.000	0.000	0.000	0.000	0.000	0.000	0.000	0.000
0.000	1.000	0.710	0.350	0.000	0.070	0.000	0.000	0.000	0.000
0.000	-0.020	1.000	0.210	0.000	-0.010	0.000	0.000	0.000	0.000
0.000	-0.010	0.040	1.000	0.000	0.000	0.000	0.000	0.000	0.000
0.000	0.060	3.760	2.340	1.000	0.170	0.000	0.000	0.000	0.000
0.000	0.280	2.360	0.550	0.000	1.000	0.000	0.000	0.000	0.000
0.000	0.000	0.000	0.000	0.000	0.000	1.000	0.000	0.000	0.000
0.000	0.000	0.000	0.000	0.000	0.000	0.000	1.000	0.000	0.000
0.000	0.000	0.000	0.000	0.000	0.000	0.000	0.000	1.000	0.000
0.000	0.000	0.000	0.000	0.000	0.000	0.000	0.000	0.000	1.000

"Converted Stripping Coefficients Matrix"

10

1.000	0.000	0.000	0.000	0.000	0.000	0.000	0.000	0.000	0.000
0.000	1.030	-0.730	-0.200	0.000	-0.070	0.000	0.000	0.000	0.000
0.000	0.020	0.980	-0.340	0.000	0.010	0.000	0.000	0.000	0.000
0.000	0.010	-0.050	1.010	0.000	0.000	0.000	0.000	0.000	0.000
0.000	-0.280	-3.230	-1.180	1.000	-0.170	0.000	0.000	0.000	0.000
0.000	-0.700	-2.120	0.260	0.000	1.030	0.000	0.000	0.000	0.000
0.000	0.000	0.000	0.000	0.000	0.000	1.000	0.000	0.000	0.000
0.000	0.000	0.000	0.000	0.000	0.000	0.000	1.000	0.000	0.000
0.000	0.000	0.000	0.000	0.000	0.000	0.000	0.000	1.000	0.000
0.000	0.000	0.000	0.000	0.000	0.000	0.000	0.000	0.000	1.000

"Sigma of Converted Stripping Coefficients Matrix"

10

0.000	0.000	0.000	0.000	0.000	0.000	0.000	0.000	0.000	0.000
0.000	0.000	-0.040	-0.017	0.000	-0.016	0.000	0.000	0.000	0.000
0.000	0.000	0.000	-0.028	0.000	0.000	0.000	0.000	0.000	0.000
0.000	0.000	-0.009	0.000	0.000	0.000	0.000	0.000	0.000	0.000
0.000	-0.080	-0.103	-0.037	0.000	-0.008	0.000	0.000	0.000	0.000

0.000 -0.140 -0.068 0.013 0.000 0.000 0.000 0.000 0.000 0.000
 0.000 0.000 0.000 0.000 0.000 0.000 0.000 0.000 0.000 0.000
 0.000 0.000 0.000 0.000 0.000 0.000 0.000 0.000 0.000 0.000
 0.000 0.000 0.000 0.000 0.000 0.000 0.000 0.000 0.000 0.000
 0.000 0.000 0.000 0.000 0.000 0.000 0.000 0.000 0.000 0.000

"Attenuation Coefficients"

10

Total	0.00600	1.00000	0.0003
K-40	0.00800	1.00000	0.0008
U-238	0.00550	1.00000	0.0114
Th-232	0.00600	1.00000	0.0044
Cs-137	0.01000	1.00000	0.0100
Co-60	0.00800	1.00000	0.0080
MMGC1	0.00600	1.00000	0.0060
MMGC2	0.00650	1.00000	0.0065
LOW	0.02000	1.00000	0.01
MID	0.01500	1.00000	0.005

"3D Attenuation Coefficients"

10

Total	0.00350	2.00000
K-40	0.00420	2.00000
U-238	0.00320	2.00000
Th-232	0.00350	2.00000
Cs-137	0.00800	2.00000
Co-60	0.00800	1.00000
MMGC1	0.00600	1.00000
MMGC2	0.00650	1.00000
LOW	0.02000	1.00000
MID	0.01500	1.00000

"Conversion factors Counts to Activity"

11

Total	0	NoCalibration	" "
K-40	7.95	AD_K-40	"Bq/kg"
U-238	3.87	AD_U-238	"Bq/kg"
Th-232	1.62	AD_Th-232	"Bq/kg"
Cs-137	1.88	AD_Cs-137	"Bq/kg"
Cs-137	32.96	AA_Cs-137	"Bq/m2"
Cs-137	7.2	AP_Cs-137	"MBq "
Co-60	2.5	AP_Co-60	"MBq "
Co-60	0	NoCalibration	" "
MMGC1	0	NoCalibration	" "
MMGC2	0	NoCalibration	" "

"Radon"

1

0 0

"Hoehenkorrektur"

3

1

1

PfadDHM25 K:\Aeroradiometrie\GammaMap\DHM25\

"SDI Constants"

7

Aten 0.0053
Convert 0.00096
CosmicKorr 95.5
Back 12640.0
Gain 12.0
referenz_alt 100.0
Threshold 240.0

----- End of file -----

Paul Scherrer Institut :: 5232 Villigen PSI :: Switzerland :: Tel. +41 56 310 21 11 :: Fax +41 56 310 21 99 :: www.psi.ch

